



저작자표시-비영리-변경금지 2.0 대한민국

이용자는 아래의 조건을 따르는 경우에 한하여 자유롭게

- 이 저작물을 복제, 배포, 전송, 전시, 공연 및 방송할 수 있습니다.

다음과 같은 조건을 따라야 합니다:



저작자표시. 귀하는 원저작자를 표시하여야 합니다.



비영리. 귀하는 이 저작물을 영리 목적으로 이용할 수 없습니다.



변경금지. 귀하는 이 저작물을 개작, 변형 또는 가공할 수 없습니다.

- 귀하는, 이 저작물의 재이용이나 배포의 경우, 이 저작물에 적용된 이용허락조건을 명확하게 나타내어야 합니다.
- 저작권자로부터 별도의 허가를 받으면 이러한 조건들은 적용되지 않습니다.

저작권법에 따른 이용자의 권리는 위의 내용에 의하여 영향을 받지 않습니다.

이것은 [이용허락규약\(Legal Code\)](#)을 이해하기 쉽게 요약한 것입니다.

[Disclaimer](#)

공학석사 학위논문

# **Ionic current modulation of gate inserted nanopores**

Gate가 삽입된 나노포어 구조에서의 이온 전류  
조절을 위한 연구

2014년 2월

서울대학교 대학원

재료공학부

여 정 모

# **Ionic current rectification in all around gate inserted nanopores**

A DISSERTATION SUBMITTED TO  
DEPARTMENT OF MATERIALS SCIENCE AND ENGINEERING  
SEOUL NATIONAL UNIVERSITY

**FOR THE DEGREE OF  
MASTER**

**Jeong Mo Yeo**

**February 2014**

## **Abstract**

Recent nanotechnology field in the past few years has accomplished a great development in bringing ion devices down to nanometer scale which as a result, the nanometer scale devices can open a new field called Nanofluidics. Nanofluidics is the study of behaviors, manipulation and control of matters that are confined to structures of nanometer scale in fluid environments. In diverse nanofluidic areas, especially, ion devices such as nanopores and nanochannel have great attentions owing to its possibility for bio/chemical analysis or sensing as platform devices. The ion devices can deal with many bio molecules or nanoparticles because nanopores and nanochannels can be worked in liquid environments in which such molecules or particles stabilized.

The two representative ion devices, nanopores and nanochannels, have several difference in geometries and characteristics. Nanochannel generally has nanometer dimension in channel cross section while the length scale is about few hundreds micro meters, so the nanochannel has a large aspect ratio. Also, nanochannels have array structures of dozens of channels and are integrated with micro channels. Usually, the nanochannel structures show better properties in ionic current rectification, also, because of the large aspect ratio, threadlike molecules such as DNA can be stretched out along the channel. On the other hand, nanopores have relatively thin thickness, less than 100nm scale with sub 10nm scale pore. In addition, the nanopore device has a membrane structure which separate reservoir into cis- and trans-chamber. The nanopore is located on the membrane and molecules and ions pass through the pore. Compare to channel structure, nanopore is relatively

easy to fabricate. Also, a single nanopore can be utilized for single molecule analysis.

One of important issues in such ion devices is to understand transport phenomena of ions, molecules or nanoparticles because understanding on transports, makes it possible to manipulate and control target molecules. Analogous to semiconductor devices, preferential ion flux can be achieved in nanofluidic devices and the ionic current rectification is caused by so called symmetry breaking of the nanofluidic system such as structure or ion concentration in ion channels. Ionic current rectification is regarded as the way of delivery of ions, particles and bio-molecules in selectively. Therefore, study on good rectifying devices is very important.

In this thesis, we suggest a fabrication method of nanopore which is characterized as all around gate structure and a very long ion channel for highly effective ionic current rectification. In order to enhance the rectification effect, we combine the nanopores with channel like structures which as a result, our nanopore is relatively very thick compare to general nanopore devices. The reason why we combine the two structures is that as mentioned above, channel shape shows better rectifying property. Also, we fabricate the nanopore that has size difference between top and bottom pore, and the asymmetrically located gate electrode around small pore region because device asymmetry is important for rectification.

The rectifying characteristic of our device will be demonstrated throughout this thesis. We expect our nanopores can give a good contribution to nanofluidic communities, since it can provide highly effective gate controllability on the ion transport.

**Keywords:** Ionic current rectification, Nanopores, Gate

**Student number:** 2012-22538

# TABLE OF CONTENTS

<b>Abstract</b> .....	i
<b>TABLE OF CONTENTS</b> .....	iv
<b>List of Figures</b> .....	vi
<b>CHAPTER 1. Introduction</b> .....	1
1.1 Ionic current modulation in solid-state nanopore system .....	2
1.2 Gate inserted nanofluidic devices: Literature Survey .....	4
1.3 Motivation.....	6
1.4 References.....	1 1
<b>CHAPTER 2. Ion transport in nanofluidic systems</b> .....	1 3
2.1 Introduction.....	1 4
2.2 Electric double layer .....	1 4
2.3 Governing equations: Poisson-Nernst-Planck equation .....	1 7
2.4 Modeling of ionic current rectification .....	1 9
2.5 Reference .....	2 4
<b>CHAPTER 3. Fabrication of gate inserted nanopore structure..</b>	2 5
3.1 Introduction.....	2 6
3.2 Membrane fabrication.....	2 6
3.3 Nanopore fabrication by Focused Ion Beam and Atomic Layer Deposition .....	2 8

<b>CHAPTER 4. Ionic current rectification of gate inserted nanopores with long ion channel.....</b>	<b>3 8</b>
4.1 Introduction.....	3 9
4.2 Results and Discussions.....	3 9
4.2.1 Results.....	3 9
4.2.2 Discussions .....	4 8
4.3 Comparison analysis .....	5 2
4.4 References.....	6 0
<b>CHAPTER5. Summary and Conclusion .....</b>	<b>6 2</b>
국문초록 .....	6 4
Acknowledgement (in Korean) .....	6 7

## List of Figures

### Chapter 1

**Figure 1.1.** Ionic current rectification in conical nanopores. The conical nanopore has a tip region (small pore area) and a base region (large pore area). The conically shaped pore shows the ionic current rectification depending on bias voltage.....7

**Figure 1.2.** Nanochannel with asymmetric bath concentration. The different ion concentration of each reservoir generates ion concentration gradient through the nanochannel. Because of the concentration gradient, the ionic current rectification can be shown depending on the bias voltage.....8

**Figure 1.3.** Gate inserted nanopores. By applying the gate potential on the nanopore wall, the ionic current can be enhanced.....9

**Figure 1.4.** The bi-polar surface charged nanochannels. The hetero-junction of different surface charged channel generates different majority charge carriers in the ion channel. In the positively charged channel, the dominant carrier is negative ion and in the negatively charged channel, the positive ion is the dominant one. Because of this difference, the dependency of ion flux on bias is appeared.....10

## Chapter 2

**Figure 2.1.** Electric double layer is a structure of accumulated counter ions near the solid surface to neutralize the surface charge caused by chemical interaction with liquid. The Electric double layer (also called Debye screening length) consists of two different layer, stern layer and diffuse layer. The stern layer is strongly fixed layer on the surface so this layer is not mobile. On the other hand, the diffuse layer is the loosely fixed layer compare to the stern layer that both the counter ions and co-ions exist even though the counter ions are dominant in the diffuse layer. Through the electric double layer, the surface charge drop to the bulk potential of solution.....21

**Figure 2.2.** Electric double layer structure in the ion channel such as nanopore or nanochannel. The total ion flux caused by ion migration is affected by both positive and negative ions. If the ion channel is dominantly occupied by electric double layer, in the channel, the contribution of counter ions on the total flux is much larger than the co-ions. Thus, because of the large volume ratio of the electric double layer, the ion channel is counter ion selective. From the figure, above device is negatively charged and has positive ion selectivity.....22

**Figure 2.3.** Schematic images of the rectifying devices which describe the mechanisms of the ionic current rectification. The symmetry breaking of structure, bath concentration or surface charges of ion device causes the inhomogeneous ion distribution in the ion channel because the ion distribution largely rely on the surface charge. Inhomogeneous ion distribution in the ion channels generates different ion flux along the position of inner channel and this different ion flux is the origin of ionic current rectification. If the flux flowing into the channel is larger than the

one flowing out of the channel, the charges are accumulated which leads to the ionic current enhancement. In contrast, if the flux flowing into the channel is less, the charge depletion takes place.....23

### Chapter 3

**Figure 3.1.** Fabrication steps for long nanopore with all around gate electrode. The step is follow as 500nm Si<sub>3</sub>N<sub>4</sub> deposition on 500um Si substrate by LPCVD, One side patterning for wet etch mask by photolithograpy, KOH wet etching for free standing Si<sub>3</sub>N<sub>4</sub> membrane, Cr electrode fabrication by e-beam lithography, 270nm Si<sub>3</sub>N<sub>4</sub> deposition, pore drilling with focused ion beam and Al<sub>2</sub>O<sub>3</sub> ALD for passivation...29

**Figure 3.2.** Schematic images of all around gate inserted nanopore with high asymmetry. The dimension of the structure is represented in the figure.....30

**Figure 3.3.** 3-dimensional image of the nanopore.....30

**Figure 3.4.** SEM images of the nanopore drilled by focused ion beam. The figure shows the top/bottom view of the pore. From this image, it can be known that there are certain size differences of the pores.....31

**Figure 3.5.** Cross section view of the pore by SEM. The gate electrode is well formed and the cross section view shows that the pore has been drilled asymmetrically. The membrane milling for cross section view is started from the bottom of the original structure shown in figure 3.2 so the electrode is located in the upper position in this image. Pt layer was coated for sample protection.....32

**Figure 3.6.** TEM image of the nanopore. This figure shows that the pore is shrunk after ALD process. Before the ALD, the pore size is about 90nm and after ALD, the pore size is about 30nm along the minor-axis. The pore shows tip size area.....32

**Figure 3.7.** The measurement setup. Ionic current is measured by Axon Patch clamp 200B. The Source-drain voltage is applied at the base region and the ground at the tip region.....33

**Figure 3.8.** Leakage current test. The leakage current test was preceded at 1M KCl concentration before the main experiment to confirm the insulation. Leakage current was measured between at the gate electrode and ground. The red line represents the floating current and the black line shows the leakage current. The result shows that leakage current is negligible.....34

## Chapter 4

**Figure 4.1.** I-V graphs of the nanopore at 1M KCl concentration. The x-axis and y-axis represents source-drain voltage and ionic current respectively. The legends show the gate voltage level. The gate effect is not significant at 1M KCl.....39

**Figure 4.2.** I-V graphs of the nanopore at 100mM KCl concentration. From the 100mM, the dependency of gate voltage on ionic current begins to be appeared. Under the positive gate potential, the ionic current is increase with gate voltage both at positive and negative source-drain voltage.....40

**Figure 4.3.** I-V graphs of the nanopore at 10mM KCl concentration. At this mole concentration, the rectification behavior can clearly be seen according to gate potential. Also, when the different gate voltage is applied, the rectification behavior is different depending on bias voltage. Rectification effect is larger under the positive gate voltage.....41

**Figure 4.4.** I-V graphs of the nanopore at 1mM KCl concentration. At this mole concentration, the rectification behavior can clearly be seen according to gate potential. Also, when the different gate voltage is applied, the rectification behavior is different depending on bias voltage. Rectification effect is larger under the positive gate voltage.....42

**Figure 4.5.** Overview of the results. The ionic current rectification depending on gate potential is shown according to mole concentration. The data is separated into two parts, positive and negative gate. Here, the scale of ionic current is not adjusted as same to emphasize the rectification trend.....43

**Figure 4.6.** The ratios of ionic current change to floating current are shown here. In order to compare the current change quantitatively, some values are extracted from the results. Every voltage value regardless of source-drain and gate voltage is the absolute 500mV. Graph(a) shows the current change according to mole concentration under the positive or negative gate voltage. The red bar is the positive gate and the blue bar is the negative gate. Graph(a) clearly shows that the ionic current increase with decrease of mole concentration and under the positive gate, the change is larger. Table (b) represents real values.....44

**Figure 4.7.** The ratio of ionic current change to floating current according to mole concentration. (a) is positive gate voltage and (b) is negative gate voltage. The maximum change is almost about 2200%. The gate voltage is +500mV and -500mV.....47

**Figure 4.8.**  $I_D$ - $V_G$  Graphs. The source drain voltage is separated into two parts; positive source-drain and negative source-drain voltage.....48

**Figure 4.9.** Device structure and ionic current change data. Nanopore on the Si<sub>3</sub>N<sub>4</sub> membrane with Cr gate has around 20nm diameter and is insulated by Al<sub>2</sub>O<sub>3</sub>. The graph shows the ratio of ionic current change to floating current according to gate voltage and the colors represent different mole concentration. Source-drain voltage was fixed as 200mV. The maximum value is about 0.1 at 1mM concentration.....52

**Figure 4.10.** Field-effect reconfigurable nanofluidic ionic diodes and I-V plot. SiO<sub>2</sub> trench was used as nanochannels. The height, width and length of the channel is respectively, 20nm, 2 $\mu$ m and 100 $\mu$ m. Gate electrode was located asymmetrically at one side. The data I-V data show preferential ion flux according to bias voltage and the diode property is different according to gate bias.....53

**Figure 4.11.** (a) Ionic transport of the nanopore IFET and gate modulation of ionic current for different KCl. (b) Schematic image of electrode-embedded nanopores for IFET and real device structure which shows multiple nanopores. The data shows clear change of ionic current according to gate voltage and the gate controllability according to mole concentration. From the results, this device has p-type like properties and the ionic current modulation is effective at the low electrolyte.....54

**Figure 4.12.** (a) The ratio of the current change to floating current is compared. The x-axis of the bar graph means each device and for convenience, number one, two and three represent respectively Derek Stein, Mark Reed and our group. From the data our device shows much effective ion modulation. (b) shows the conductance change compare to floating conductance. The one on the left side is Nam's data and the other is our data.....55

**Figure 4.13.** (a) The simulation data according to surface charge, gate position and gate voltage. (b) shows comparison the ionic current curve with the simulation data reported by Shizhi Qian at al. Red symbol represents positive gate and blue is negative gate. Source-drain voltage of the two data is applied in opposite way.....56

## **CHAPTER 1. Introduction**

## **1.1 Ionic current modulation in solid-state nanopore system**

Over the past several decades, nanofluidic area including nanopores and nanochannels has been widely developed owing to its promising potentials for biological and chemical applications.[1] Among many nanopore applications, solid-state nanopores are the one of growing scientific interest because the solid-state device present very high stability, controllability of nanopore geometries and adjustable surface properties compare to biological nanopores. [2] Also, synthetic nanopores from solid-state materials can be utilized for various lab-on-a-chip applications which make it possible to integrate a system of sample collection, transport and separation for biological and chemical specimens on a tiny miniaturized chip. [3] On the point of the integration and bio molecule analysis, ionic current regulation is very important characteristic because the ionic current control is regarded as the way of delivery of chemical species as we want and by controlling ionic current, nanofluidic logic circuit can be utilized like solid-state semiconductor technology. One of interesting phenomena is the ionic current rectification effect which shows preferable ion flows depending on bias voltage. By using the rectification, diverse transports phenomena of molecules and polymers can be understood. Therefore, it is worth noting that study on ionic current behavior and fabrication of rectifying devices in nanofluidic system can open new windows for biological and chemical analysis.

In previous studies, several fabrication methods in order to make devices which show the ionic current rectification have been developed such as, conical [4], asymmetric bath concentration [5], bi-polar surface

charged nanopores [6] [7] and gate electrode embedded structure. [8] The rectification phenomenon shown in above structures is originated from broken symmetry of nanopore system such as geometries and charge distribution, because the asymmetry can causes certain cation/anion ratio in the pore or channel and the difference between positive and negative ion concentration give rise to the ion permselectivity. [9] Disproportionately distributed ion concentration makes the preferable ion fluxes possible. Not only the fact mentioned above, but also surface charge of the nanopore wall is very important factor to explain the rectification effect and total ion flux in nanofluidic system, because the ion flux is significantly affected by surface charge. [10],[11] Especially important point is that surface charge leads to forming Electric Double Layer (EDL) in order to screen the surface charge in the vicinity of the liquid/pore wall interface and the screening layer has huge effect on the ion flux when the dimension of pore or channel becomes nanoscale or comparable to the EDL for that electrolyte. A typical example of ionic current rectification affected by broken symmetry and surface charges is the conical nanopores which has large asymmetry between tip and base opening. In the conical nanopore system, the Debye Screening Length can be comparable near the tip opening in low salt concentration and the tip region becomes very ion-selective, so the conical structure shows high ionic current rectification. Therefore, the asymmetry in geometries, surface charge distributions and bath concentrations is the key for the current rectification.

## 1.2 Gate inserted nanofluidic devices: Literature Survey

Ionic field effect transistor type nanopores can also regulate the ion flux, and this controlled ionic current by gate voltage has advantage over the other methods mentioned above section, because those devices have predefined rectifying property while the electric field effect type can shows a switchable ionic current property. In the gated nanopore, gate potential imposed on the pore wall will be a key parameter for the rectified ion transport analogous to Metal-Oxide-Semiconductor Field Effect Transistor (MOSFET) devices. The fundamentals of explanation of the ionic current rectification is the same as well. Applied potential on the gate can change the surface state of the pore wall which as a result, ion accumulation and depletion can be formed according to gate voltage and this will generate ionic current rectification. Because of large dependency of ion flux on gate voltage, ionic current can be easily controlled. Therefore, nanopore with the inserted gate electrode may provide a rapid and flexible nanofluidic device for ionic current regulation.

Nam *et al* report the multiple nanopore structures with sub-10 nm diameter for electrofluidic applications which demonstrate an ionic gating process. [12] Modulation of ionic conductivity of the nanopores according to  $V_G$  was clearly represented and in particular, at low mole concentration, this ionic field effect transistor shows the unipolar current increases under negative gate potential like p-PET devices which means that the nanopores was occupied by positive ions. Also, in another paper, the effect of surface charge density on the ion conductance and its dependence on the applied gate field of  $Al_2O_3$  nanopore transistors was

described. [13] These two reports show the clear evidence of the electric field effect control over the ion conductance. Not only gate potential, but also position of the gate electrode in the nanopore can affect ionic current behavior. Especially, the asymmetrically located gate electrode can regulate the forward/reverse directions by gate voltages as well as diodes. [14] In this paper, it is revealed that the ionic current polarity was only shown in the asymmetric gate device. However, in case of mid-positioned gate device did not show the preferential ionic current but Ohmic enhancement of the amount of current under gate potential.

### 1.3 Motivation

So far, Ionic current regulation can be achieved by several fabrication methods. However, the multi-pores[12] might be a challenge to analyze a single molecule and cost a lot. In addition, the ion manipulation effectiveness of the above mentioned  $\text{Al}_2\text{O}_3$  [13] or the nanochannel with asymmetrically positioned gate[14] seems not that high. Hence, we have tried to fabricate gated nanopores which show more effective ionic current regulation and has single pore with convenience to fabrication.

In this article, we suggest the single nanopore device with asymmetrically located gate electrode in order to investigate the ionic current modulation. Our nanopore device, unlike the existing gated nanopores, has relatively thick membrane but thin gate electrode in order to make highly broken symmetry and enhance the current controllability. Even with the single nanopore, our pore shows the better ion manipulation property. We have fabricated the nanopore device with 30nm diameter and 800nm thickness. The 30nm thick gate electrode was inserted around 200nm position from the bottom of the pore so that the electrode can be positioned asymmetrically and we believe this thin and asymmetrically located electrode can cause the current rectification. In this paper, we will represent that the results about the electrical properties of our nanopore according to gate potential and ion concentration.

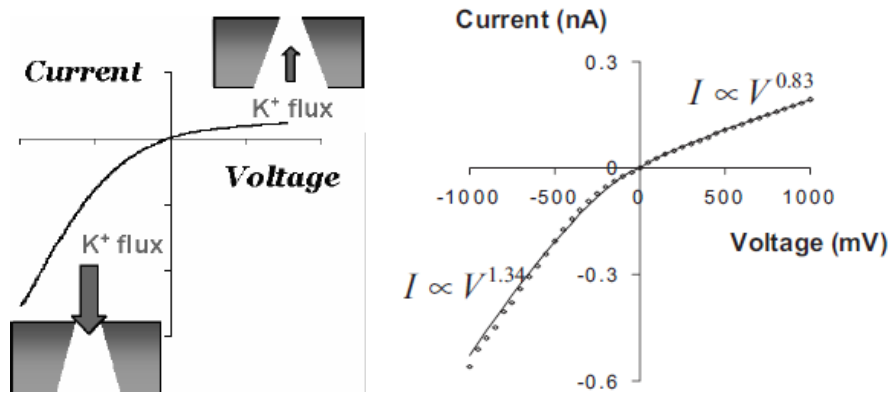


**Figure 1.1.** Ionic current rectification in conical nanopores. The conical nanopore has a tip region (small pore area) and a base region (large pore area). The conically shaped pore shows the ionic current rectification depending on bias voltage.[4]

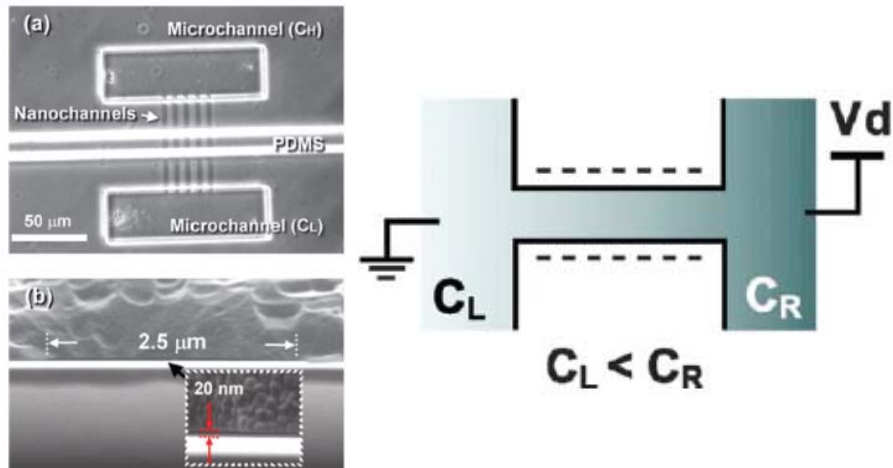


**Figure 1.2.** Nanochannel with asymmetric bath concentration. The different ion concentration of each reservoir generates ion concentration gradient through the nanochannel. Because of the concentration gradient, the ionic current rectification can be shown depending on the bias voltage.[5]

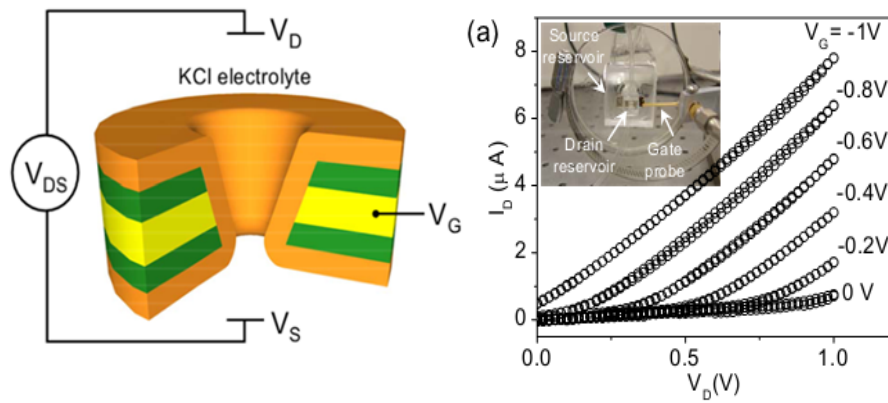


**Figure 1.3.** Gate inserted nanopores. By applying the gate potential on the nanopore wall, the ionic current can be enhanced.[12]

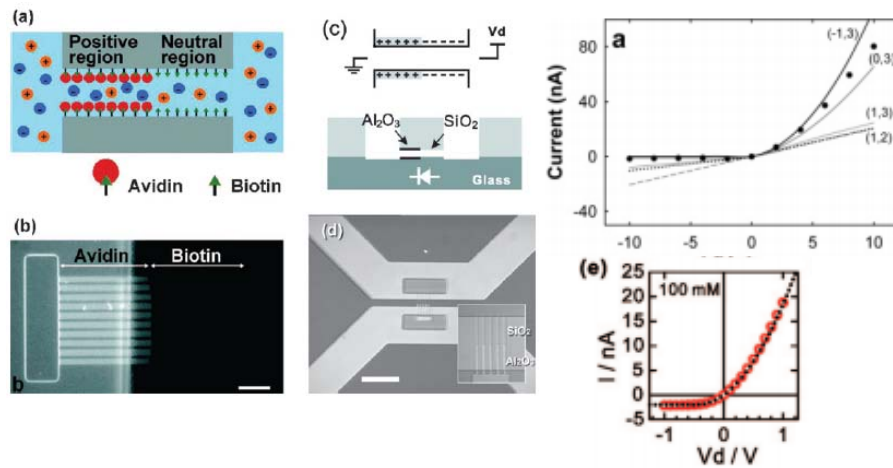


**Figure 1.4.** The bi-polar surface charged nanochannels. The hetero-junction of different surface charged channel generates different majority charge carriers in the ion channel. In the positively charged channel, the dominant carrier is negative ion and in the negatively charged channel, the positive ion is the dominant one. Because of this difference, the dependency of ion flux on bias is appeared.[15]

## 1.4 References

1. Branton, D., et al., *The potential and challenges of nanopore sequencing*. Nat Biotechnol, 2008. **26**(10): p. 1146-53.
2. Dekker, C., *Solid-state nanopores*. Nat Nano, 2007. **2**(4): p. 209-215.
3. Manz, A., N. Graber, and H.M. Widmer, *Miniaturized total chemical analysis systems: A novel concept for chemical sensing*. Sensors and Actuators B: Chemical, 1990. **1**(1-6): p. 244-248.
4. Siwy, Z.S., *Ion-Current Rectification in Nanopores and Nanotubes with Broken Symmetry*. Advanced Functional Materials, 2006. **16**(6): p. 735-746.
5. Cheng, L.-J. and L.J. Guo, *Rectified Ion Transport through Concentration Gradient in Homogeneous Silica Nanochannels*. Nano Letters, 2007. **7**(10): p. 3165-3171.
6. Daiguji, H., Y. Oka, and K. Shirono, *Nanofluidic Diode and Bipolar Transistor*. Nano Letters, 2005. **5**(11): p. 2274-2280.
7. Karnik, R., et al., *Rectification of Ionic Current in a Nanofluidic Diode*. Nano Letters, 2007. **7**(3): p. 547-551.
8. Fan, R., et al., *Polarity Switching and Transient Responses in Single Nanotube Nanofluidic Transistors*. Physical Review Letters, 2005. **95**(8).
9. Cheng, L.J. and L.J. Guo, *Nanofluidic diodes*. Chem Soc Rev, 2010. **39**(3): p. 923-38.
10. Stein, D., M. Kruithof, and C. Dekker, *Surface-Charge-Governed Ion Transport in Nanofluidic Channels*. Physical Review Letters, 2004. **93**(3): p. 035901.

11. Daiguji, H., P. Yang, and A. Majumdar, *Ion Transport in Nanofluidic Channels*. Nano Letters, 2003. **4**(1): p. 137-142.
12. Nam, S.-W., et al., *Ionic Field Effect Transistors with Sub-10 nm Multiple Nanopores*. Nano Letters, 2009. **9**(5): p. 2044-2048.
13. Jiang, Z. and D. Stein, *Charge regulation in nanopore ionic field-effect transistors*. Physical Review E, 2011. **83**(3).
14. Guan, W., R. Fan, and M.A. Reed, *Field-effect reconfigurable nanofluidic ionic diodes*. Nat Commun, 2011. **2**: p. 506.
15. Rohit Karnik and Arun Majumdar, *Rectification of fluidic current in a nanofluidic diode*. Nano Letters, 2007. 21 p: 547-551

## **CHAPTER 2. Ion transport in nanofluidic systems**

## **2.1 Introduction**

Understanding on diverse transport phenomena is important for utilizing the nanofluidic devices effectively. Electrokinetic transports of bio-molecules or nanoparticles are very important issues and this field is intensively being investigated. This is because the ion transport is closely related to deliveries of bio molecules or ions. Also, when it comes to basic properties of nanofluidic devices, the ion transport is the one of main characteristics of the devices. This ion or electrokinetic transports is heavily affected by surface charges of the nanopore or nanochannel. Here, I am going to explain some background knowledge for the underlying principles on the ion transport.

## **2.2 Electric double layer**

Electric double layer (EDL) is an ion accumulation formed at an interface of an object contacted with liquid. Generally, the object is a solid material like nanoparticles and when the solid object is into a liquid, surface charges are formed at the surface due to chemical interactions. Because of this surface charge, counter ions can be accumulated near the surface to meet the charge neutrality and the accumulated ion layer is called Electric Double Layer (also called Debye Screening Length). The EDL has ranges from few nanometers to hundreds and plays an extremely important role in systems with a large surface area to volume ratio such as nanopores, nanochannels which are in micrometer to nanometer range. For example, in the nanopore systems, the surface area ratio to its volume is very high, so the EDL size is comparable to the pore. Thus, the electric double layer has effects on the diverse nanofluidic

phenomena and in many case, it is relate to transport phenomena such as ion and electrokineic transports of particles and molecules. Generally, the EDL can influence the electric potential in systems. The thickness of EDL can be deduced from the Poisson-Boltzmann equation with Debye-Huckel approximation.[1]

$$\nabla^2\psi = \frac{d^2\psi}{dz^2} = \kappa^2\psi(z)$$

where

$$\kappa = \left( \frac{e^2 \sum_i c_i z_i^2}{\varepsilon_0 \varepsilon_r k_B T} \right)^{1/2}$$

$\kappa$  is called as the Debye-Huckel parameter which is the inverse of the EDL.  $c_i$  represents the ion concentration of  $i$  species ion. One important effect of the EDL is that this layer makes ion selectivity in the nanofluidic systems.

As mentioned above, the electric double layer consist of mainly counter ions even though there are few co-ions exist too, so the EDL is the counter ion reach region. For example, if the surface is negatively charged, the EDL is dominantly occupied by positive ions. In this situation, if the device size like a nanopore is comparable to the electric double layer, the pore can be dominantly filled with counter ions. Then the ion flux can be mainly composed of counter ions. Here is an example of this phenomenon. If the nanopore is small enough to be occupied by EDL and negatively charged, this pore transports the positive ions

dominantly with certain selectivity, which means that the negative ions cannot be well pass through the pore. The certain ion ratio is shown by[2][3]

$$\alpha = \frac{\bar{c}_+}{\bar{c}_-} = \left( \frac{-f + \sqrt{f^2 + 4c_b^2}}{2c_b} \right)^2$$

where,

$$f = \frac{2\sigma_s 10^{-3}}{qN_A h}$$

$\sigma_s$  is the surface charge density and the  $h$  means the structural factor. In this case, the  $h$  is the height of nanochannels.

### 2.3 Governing equations: Poisson-Nernst-Planck equation

In order to describe the motion of chemical species in a fluid medium, people employ the Nernst-Planck equation which describes the total ion flux. The ion flux can be driven by both concentration gradient and electric potential. In addition, convection of the fluid medium affects the total migration and this can be described by the Navier-Stokes equation. With these two equations and the Poisson equation, almost of all informations for describing nanofluidic systems can be obtained. Nernst-Planck equation is represented by[4]

$$\vec{J}_i = -\mu_i z_i e F c_i \nabla \phi - D_i \nabla c_i + c_i \vec{v}$$

The first term on the right side of the equation shows the drift term driven by electrical potential and second term is about concentration gradient. The last one is the contribution of convection flow. The contribution of fluid flow can be neglected when the entire region of the nanopores or nanochannel are dominantly occupied by EDL. However, if there is some space which acts like bulk solution, the convection term can be taken account for the ion flux. The fluid velocity can be obtained by simplified Navier-Stokes equation due to the nature of nanofluidic systems

$$\mu \nabla^2 \vec{v} = -\rho E$$

where  $\mu$  is mobility of ions and  $\rho, E$  is respectively charge density and

electric potential. From this equation the velocity of fluid is shown by

$$\vec{v}_x(y) = -\frac{\epsilon\zeta}{\mu} E_x$$

where  $\zeta$  is zeta potential. This is called as Helmholtz-Smoluchowski velocity. From the Nernst-Planck equation, the ion distribution can be obtained by

$$n_i = n^\infty \exp\left[-\frac{z_i e}{kT} \psi \parallel_{surface}\right]$$

Through this relationship, it can be known that the ion distribution follows Boltzmann Distribution.

## 2.4 Modeling of ionic current rectification

Analogous to the solid-state semiconductor devices, in nanofluidic systems, a preferential ion transport can be utilized. This preferential ion flux shows diode behavior and makes a forward state which is the ionic current enhancement and a reverse state. This phenomenon is called ionic current rectification and the rectification is obtained, as continuously said through this article, by several fabrication methods such as conical nanopores, asymmetric bath concentration type and bi-polar surface structured nanochannels. For instance, similar to P-N junction of semiconductor, the hetero-junction of two different surface charged nanochannels can generate the diode property depending on applied bias because the two different nanochannel is occupied by different majority carriers. To be specific, when positive major carrier and negative major carrier is separated at the interface of hetero-junction, the forward bias should be applied at the positive majority region and the ground should be at the negative rich region.

In the previous studies,[2] researchers use a term called ‘symmetry breaking of the systems’ to explain the ionic current rectification. The symmetry breaking means that the nanofluidic devices have certain broken symmetry of structure, surface charges or ion distribution. For example, above the bi-polar surfaced ion device has the symmetry breaking in surface charges because the surface charge through the entire channel is not homogeneous but heterogeneous. Also, according to the paper, the ionic current rectification effect becomes larger if the symmetry breaking is big.

The schematic image of figure 2.3 shows the mechanism of the ionic current rectification in each device. A conical nanopore, asymmetric bath concentration type and the bi-polar surface charged nanochannel is represented respectively. For more details, I am going to depict another structure which has the structural symmetry breaking, conical nanopore. In case of conical nanopore, there is some concentration difference between the tip region (small pore sized area) and the base region (large pore sized area) because the tip region is small enough to be comparable to the electrical double layer yet, the base region is larger than EDL. In this case, the tip region is more ion selective for positive ion as shown in the figure 2.3(1). So if the drain voltage is applied at the tip region and the ground is at the base region (figure 2.3(1b)), the ion flux flowing into the channel due to the positive ion is large at the tip region and the flux flowing out of the channel is small, thus, the charges can be accumulated in the channel because of the flux difference. Therefore, this case shows the forward bias which means that the ionic current can be enhanced. On the other hand, if the reverse bias is applied to the conical pore (figure 2.3(1c)), the flux flowing out of the pore is bigger than the one flowing into the pore, so the ionic current is depleted

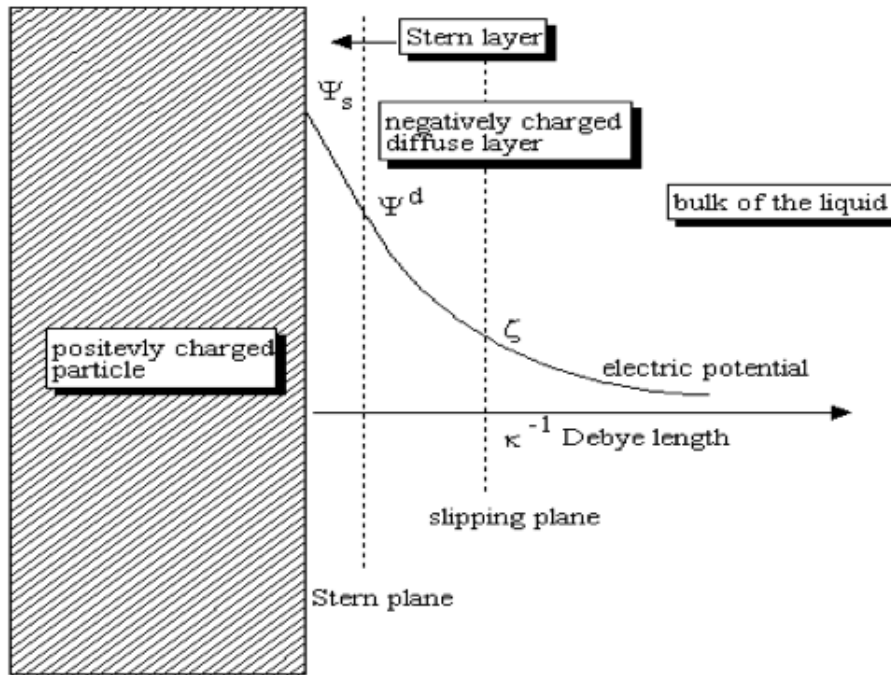


**Figure 2.1.** Electric double layer is a structure of accumulated counter ions near the solid surface to neutralize the surface charge caused by chemical interaction with liquid. The Electric double layer (also called Debye screening length) consists of two different layer, stern layer and diffuse layer. The stern layer is strongly fixed layer on the surface so this layer is not mobile. On the other hand, the diffuse layer is the loosely fixed layer compare to the stern layer that both the counter ions and co-ions exist even though the counter ions are dominant in the diffuse layer. Through the electric double layer, the surface charge drop to the bulk potential of solution.

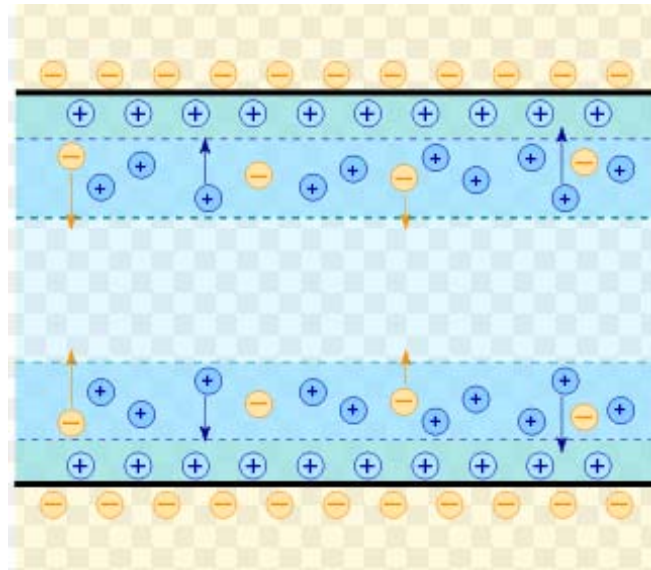


**Figure 2.2.** Electric double layer structure in the ion channel such as nanopore or nanochannel. The total ion flux caused by ion migration is affected by both positive and negative ions. If the ion channel is dominantly occupied by electric double layer, in the channel, the contribution of counter ions on the total flux is much larger than the co-ions. Thus, because of the large volume ratio of the electric double layer, the ion channel is counter ion selective. From the figure, above device is negatively charged and has positive ion selectivity.

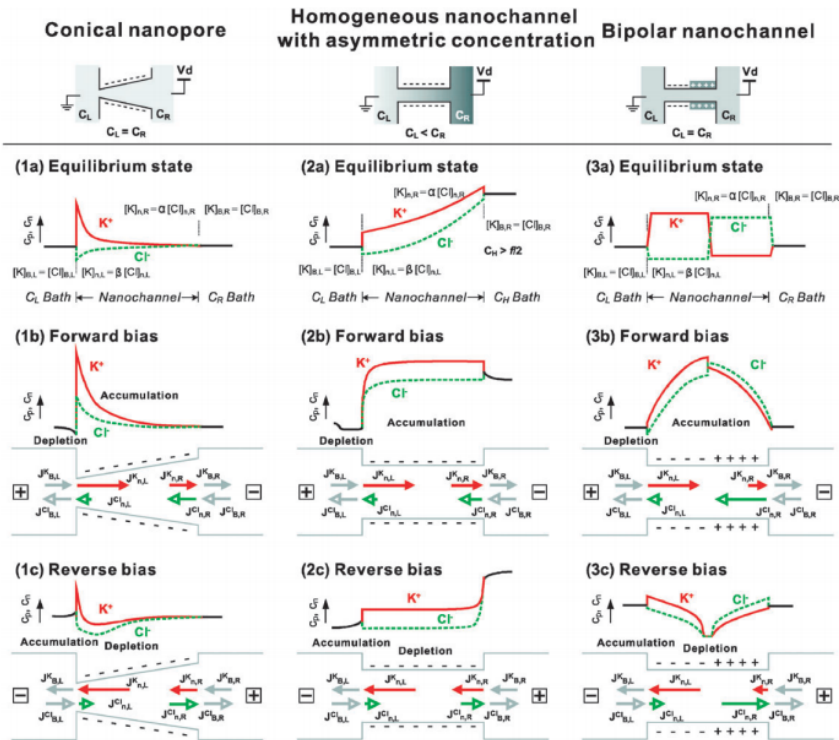


**Figure 2.3.** Schematic images of the rectifying devices which describe the mechanisms of the ionic current rectification. The symmetry breaking of structure, bath concentration or surface charges of ion device causes the inhomogeneous ion distribution in the ion channel because the ion distribution largely rely on the surface charge. Inhomogeneous ion distribution in the ion channels generates different ion flux along the position of inner channel and this different ion flux is the origin of ionic current rectification. If the flux flowing into the channel is larger than the one flowing out of the channel, the charges are accumulated which leads to the ionic current enhancement. In contrast, if the flux flowing into the channel is less, the charge depletion takes place. [2]

## 2.5 Reference

1. Reto B. Schoch, *Transport phenomena in nanofluidics*. Rev Mod Phys, 2008. **80**(3): 6861
2. Cheng, L.J. and L.J. Guo, *Nanofluidic diodes*. Chem Soc Rev, 2010. **39**(3): p. 923-38.
3. G. Stell and C.G. Joslin, *The donnan equilibrium a theoretical study of the effects of interionic forces*. Biophysical society, 1986. **50**: p. 855-859
4. W. Sparreboom, *Transport in nanofluidic systems: a review of theory and applications*. New Journal of Physics, 2010. **12** p. 23
5. Hirofumi Daiguji, *Ion transport in nanofluidic channels*, Chem. Soc. Rev, 2010. **39**: 901-911
6. Li-Jing Cheng and L. Jay Guo, *Rectified ion transport through concentration gradient in homogeneous silica nanochannels*, 2007. **7** p: 3165-3171
7. Eric B. Kalman and Zuzanna S. siwy, *Control of ionic transport through gated single conical nanopores*, Anl Bioanal Chem, 2009. **394** 413-419

## **CHAPTER 3. Fabrication of gate inserted nanopore structure**

### **3.1 Introduction**

Now, in this chapter, I will show the fabrication method step by step. Again, our purpose is to make very asymmetric structure for all above mentioned reasons. Our final device structure has asymmetry in tip and base pore, so the cross section view of the nanopore looks like funnel or conical structure (figure 3.2). This can be seen in figure 3.5. Plus, the electrode is also asymmetrically positioned and localized at small pore region (figure 3.5). Note that the reason why the electrode is located at upper pore (figure 3.5) which has bigger pore size is the limitation of Focused Ion Beam measurement. In the FIB instrument, the angle between SEM probe and FIB probe is 56 degree which as a result, the cross section view cannot be seen from the etched Si substrate side because of angle between the etched Si planes. Hence, we just measure the cross section view from the top of the membrane. Figure 3.2 may help you understand.

### **3.2 Membrane fabrication**

The  $\text{Si}_3\text{N}_4$  membrane was fabricated by the conventional method on the Si substrate. The nanochannel used in this article was fabricated in free standing triple layer, 500nm thick silicon nitride, 30nm Cr and 200nm  $\text{Si}_3\text{N}_4$  membrane supported by 300 $\mu\text{m}$  thick silicon wafer (Si 100) using Focused Ion Beam (FIB).  $\text{Si}_3\text{N}_4$  was deposited on the double polished Si wafer by Low-Pressure Chemical Vapor Deposition(LPCVD) and was patterned by photolithography(MA6II Aligner) with a 750 $\mu\text{m}$   $\times$  750 $\mu\text{m}$  square window exposed for KOH wet etching then the finally 50 $\mu\text{m}$  opening size of the membrane was obtained. Before the KOH

etching, the patterned  $\text{Si}_3\text{N}_4$  layer was etched by Reactive Ion Etching (RIE, Oxford) in order to exposure the bare Si surface for the wet etching. (Dry etching conditions;  $\text{CF}_4$  gas flow, pressure, power and etching time was respectively 50sccm, 0.03torr, 100W and 15min). Then, the KOH wet etching was carried out to etch the Si substrate at  $80^\circ\text{C}$  for 10hours and then we obtained free standing 500nm  $\text{Si}_3\text{N}_4$  membrane. After fabricated the membrane, we deposited patterned 30nm thick Cr layer on the membrane as a gate electrode by E-beam evaporation and used lift-off method to obtain patterned chromium layer. Next step was to deposit the other  $\text{Si}_3\text{N}_4$  layer on top of the former membrane by Plasma Enhanced Chemical Vapor Deposition (PECVD). Final membrane was layer by layer, 500nm  $\text{Si}_3\text{N}_4$ , 30nm Cr and 200nm  $\text{Si}_3\text{N}_4$ , so the total thickness was about 730nm. Then the electrode was exposed by RIE to apply gate voltage.

### **3.3 Nanopore fabrication by Focused Ion Beam and Atomic Layer Deposition**

After all of those steps, we drilled nanopore by using Focused Ion Beam (FIB) and conducted aluminum oxide ( $\text{Al}_2\text{O}_3$ ) Atomic Layer Deposition (ALD) to make the dielectric layer for gating and again the oxide layer should be removed for metal contact by dilute hydrofluoric acid (DHF) for 2min. The final nanopore structure is not perfectly cylindrical but has some asymmetry owing to the sputtering like property of the FIB so it has funnel like pore shape rather than the cylinder.

FIB (Focused Ion Beam, AURIGA Carl Zeiss) machine use Ga ion as a source for a patterning. Beam patterning or milling principle is that a finely focused beam of ions which is operated by the FIB system can be employed for imaging or site specific sputtering or milling. The gallium ion beam hits the sample surface and sputters a small amount of materials and through this collision event, a specific pattern or milling can be achieved. So the ion beam can be focused on the membrane and by using the beam sputtering, the nanometer sized hole can be fabricated. The FIB instrument used in the experiment has the 9nm spot size to beam sputtering and the beam spot is rendering to hit the surface. The nanopore size and structure highly depends on the beam intensity and parameters for the ion beam are acceleration voltage and beam current level. Once the voltage and current is fixed, by setting target size for the beam exposure area and dose, the final pore is fabricated. If the sputtering energy is not sufficient, the membrane cannot be drilled at all so, the optimum condition should be determined and at a certain condition, the nanopore can be drilled like a conical structure. In order to confirm this

fact, SEM analysis was done. The figure shows that the top/bottom image of the pore and from this image, the pore size of the top/bottom can be different. Also, Gate structure needs a good dielectric layer to impose gate potential onto the ion channel so the ALD (Atomic Layer Deposition) method were used to deposit  $\text{Al}_2\text{O}_3$  layer on the nanopore wall. Our oxide layer has very low surface charge density from the zeta-potential measurement.

Before measure the ionic current with this device, the sample was wetted for more than 1 hour in the high purity ethanol. PDMS chamber was filled with ionic solution, KCl, and the  $1\text{cm} \times 1\text{cm}$  sample was loaded on top of this chamber. In addition, in order to verify the dielectric layer quality, leakage test was preceded. Two Ag/AgCl electrodes were inserted into the two reservoirs respectively, and connected to the Axon Patch-clamp 200B. Ionic current was measured according to mole fraction and gate potential. The mole fraction changes were respectively, 100mM, 10mM and 1mM KCl. Also, the gate voltages were changed from -500mV to 500mV and the increment was 100mV. The gate voltage was fixed and the source-drain voltage was swept.

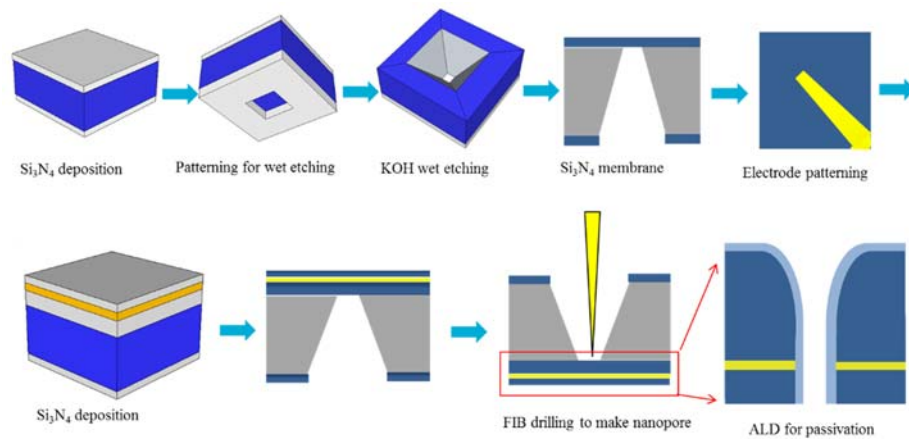


**Figure 3.1.** Fabrication steps for long nanopore with all around gate electrode. The step is follow as 500nm Si<sub>3</sub>N<sub>4</sub> deposition on 500um Si substrate by LPCVD, One side patterning for wet etch mask by photolithograpy, KOH wet etching for free standing Si<sub>3</sub>N<sub>4</sub> membrane, Cr electrode fabrication by e-beam lithography, 270nm Si<sub>3</sub>N<sub>4</sub> deposition, pore drilling with focused ion beam and Al<sub>2</sub>O<sub>3</sub> ALD for passivation.

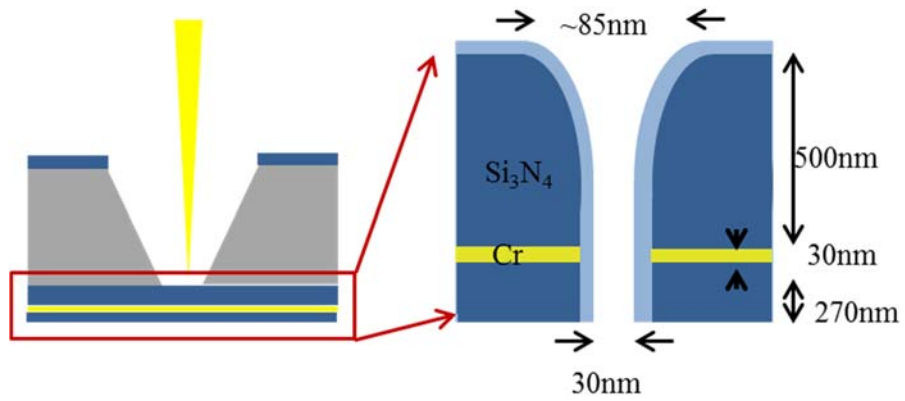


**Figure 3.2.** Schematic images of all around gate inserted nanopore with high asymmetry. The dimension of the structure is represented in the figure.

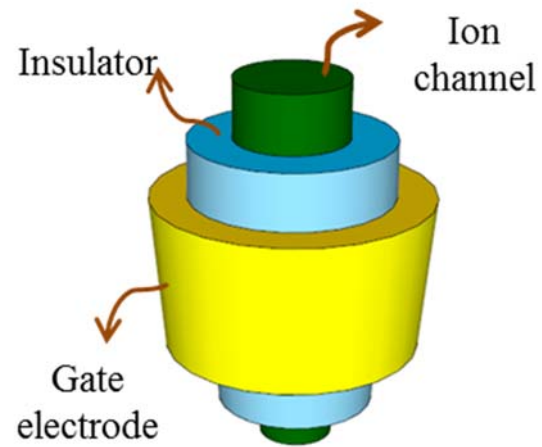


**Figure 3.3.** 3-dimensional image of the nanopore

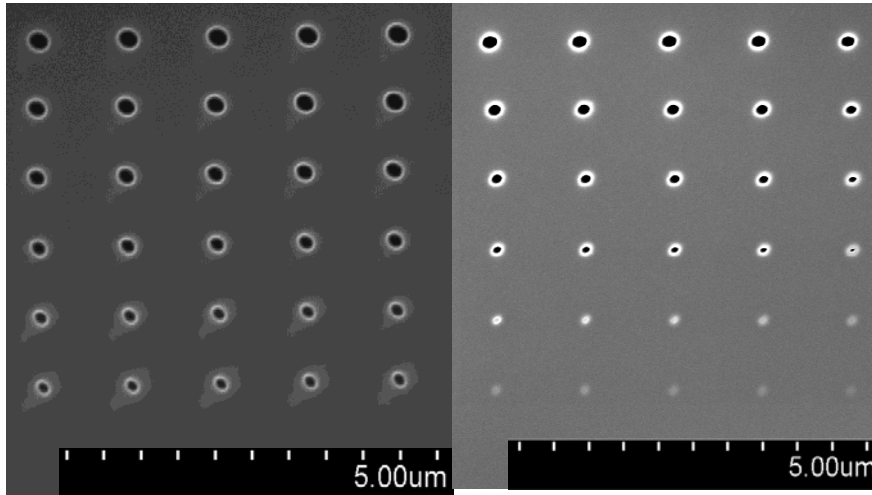


**Figure 3.4.** SEM images of the nanopore drilled by focused ion beam. The figure shows the top/bottom view of the pore. From this image, it can be known that there are certain size differences of the pores.

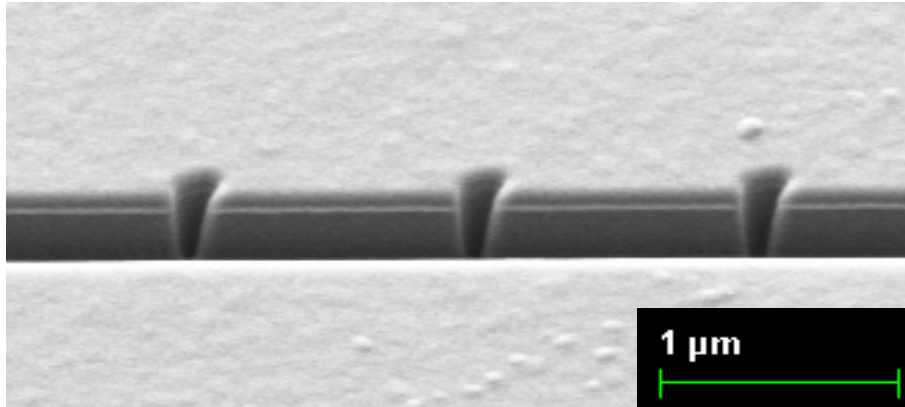


**Figure 3.5.** Cross section view of the pore by SEM. The gate electrode is well formed and the cross section view shows that the pore has been drilled asymmetrically. The membrane milling for cross section view is started from the bottom of the original structure shown in figure 3.2 so the electrode is located in the upper position in this image. Pt layer was coated for sample protection

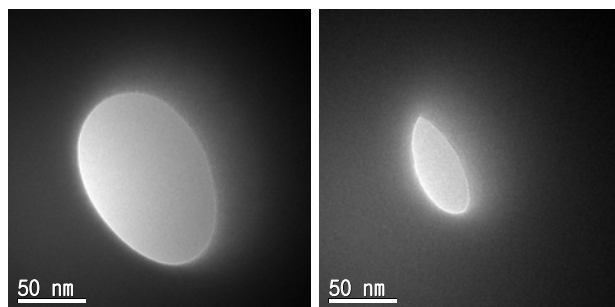


**Figure 3.6.** TEM image of the nanopore. This figure shows that the pore is shrunk after ALD process. Before the ALD, the pore size is about 90nm and after ALD, the pore size is about 30nm along the minor-axis. The pore shows tip size area

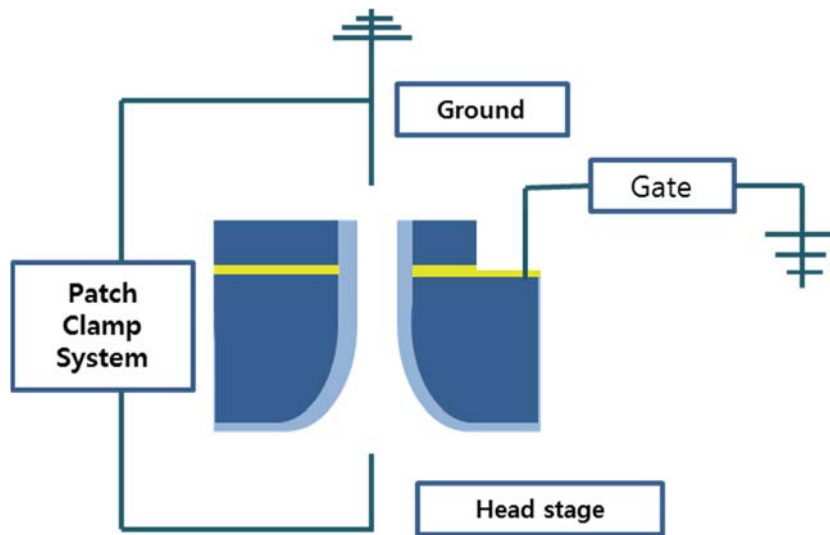


**Figure 3.7.** The measurement setup. Ionic current is measured by Axon Patch clamp 200B. The Source-drain voltage is applied at the base region and the ground at the tip region

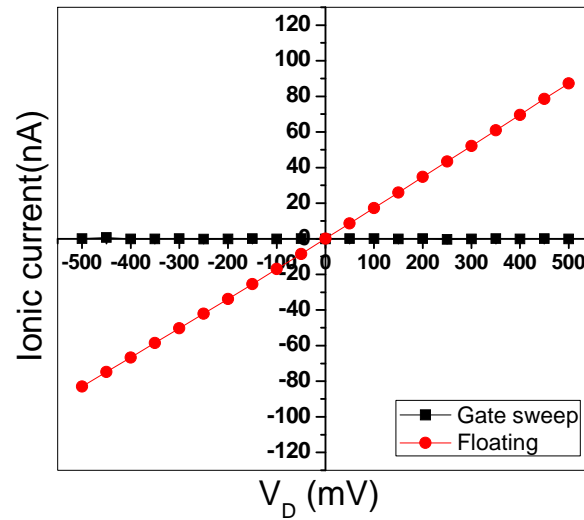


**Figure 3.8.** Leakage current test. The leakage current test was preceded at 1M KCl concentration before the main experiment to confirm the insulation. Leakage current was measured between at the gate electrode and ground. The red line represents the floating current and the black line shows the leakage current. The result shows that leakage current is negligible

**CHAPTER 4. Ionic current rectification of gate inserted nanopores with long ion channel.**

## **4.1 Introduction**

We investigated the effect of gate voltage on the ionic current characteristics according to ion strength. Each gate voltage was fixed and source-drain voltage was swept from -500mV to 500mV. The data is separated into two parts, positive and negative gate potential. So, we could recognize the gate effect on I-V characteristics depending on its signs. Our data shows different polarity of ionic current between positive and negative gate voltage. Under the positive gate voltage, ionic current enhancement, the forward current, is shown at negative source-drain voltage region but reverse state is occurred at positive drain voltage. (figure 4.3(a)) At the forward state, drastic increase of ionic current is observed. In contrast, under the negative gate potential (figure 4.3(b)), the forward state is occurred at positive drain voltage.

## **4.2 Results and Discussions**

### **4.2.1 Results**

First, 1M concentration KCl data was shown in figure 4.1 and the results is separated into two parts, positive and negative gate potential. In this result, the measured pore is not the same so the conductance is different. Except pore diameter, the other structure is exactly the same as shown in fabrication section. Thus, these two devices can be directly compared to each other and show the gate effect on ionic current. The total ionic current level is about nano-ampere range. The x-axis of the I-V graphs shown in figure 4.1 represents source-drain voltage and the y-axis means ionic current. The different colors shown in the legends

represent different gate potential levels. As clearly shown in the graphs, there are no significant changes according to the gate voltage at both positive and negative gate. In order to compare quantitatively, couple of current change values were extracted from the results and shown in the table of figure 4.6(b). All the values are about 1 and there is no big difference.

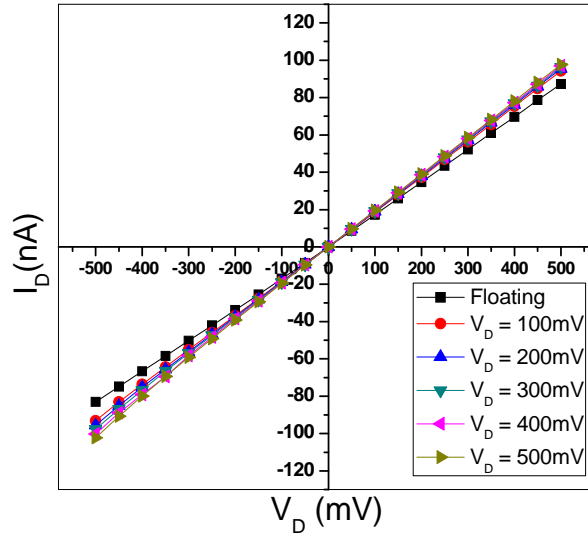
Second results show the I-V curves at 100mM concentration (figure 4.2) and these are separated in the same way as well as the 1M data. From this data, the dependency of ionic current on gate potential begins to be seen. As the gate potential gets increased, the ionic current level is enhanced through the entire source-drain voltage region under the positive gate voltage yet, the amount of enhancement is higher at the negative drain voltage than at the positive one. Also, under the negative gate voltage, the ionic current is increased according to the gate voltage at positive source-drain voltage. However, at the negative drain voltage, there is no big change. Here, the ionic current change value is shown too in the table of figure 4.6(b). From the I-V graphs and the real values, it can be noticed that there is some enhancement gap between positive and negative gate potential.

A distinctive change from the above results begins to be appeared at the 10mM concentration KCl (figure 4.3). From this mole concentration, the rectification behavior can clearly be seen according to the gate voltages. A look at the positive gate potential shows that the forward state of the ionic current is shown under the negative source-drain voltage and at the negative source-drain voltage, the ionic current is reverse state. On the other hands, under the negative gate voltage, the forward state is shown at the positive source-drain voltage. The table of

figure 4.6(b) represents the ionic current changes and each forward shows definitely bigger ionic current enhancements.

Finally, at the 1mM concentration (figure 4.6), the rectifying behavior is shown as well as at the 10mM and the trend according to the gate potential is exactly the same. The increment of ionic current at the forward state is the biggest. The above current change according to each mole concentration is shown in the figure 4.5 and as can be seen in this figure, the amount of ionic current change is enhanced with decrease of mole concentration. Also, the gate controllability is higher under the positive gate voltage.

(a)



(b)

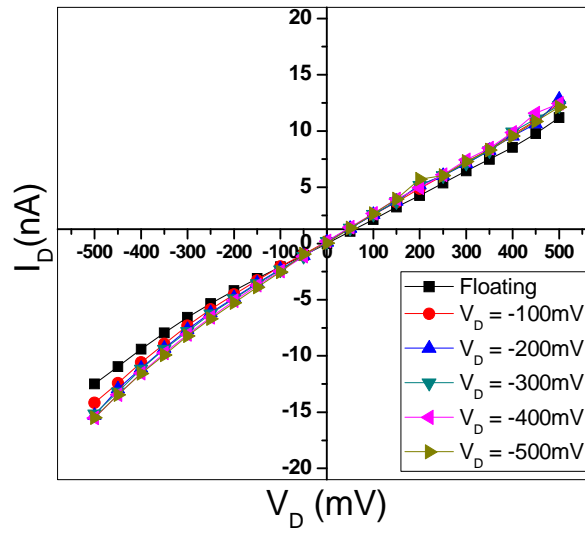
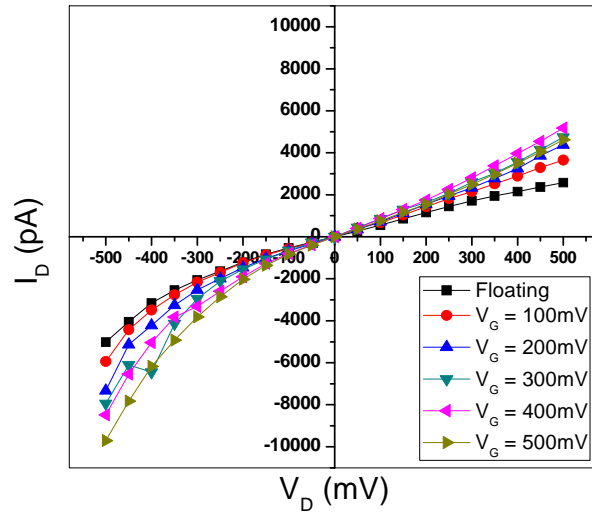


**Figure 4.1.** I-V graphs of the nanopore at 1M KCl concentration. The x-axis and y-axis represents source-drain voltage and ionic current respectively. The legends show the gate voltage level. The gate effect is not significant at 1M KCl. (a) is positive gate, (b) is negative gate

(a)



(b)

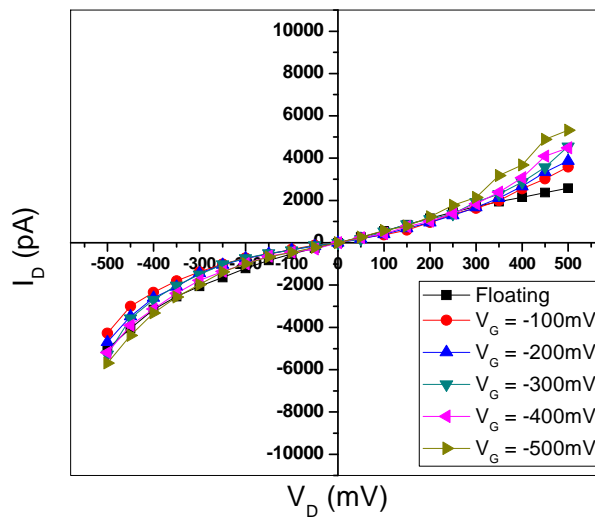
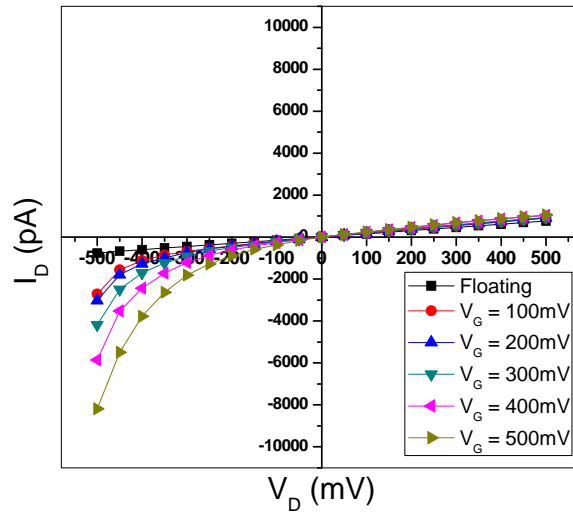


**Figure 4.2.** I-V graphs of the nanopore at 100mM KCl concentration. From the 100mM, the dependency of gate voltage on ionic current begins to be appeared. Under the positive gate potential, the ionic current is increase with gate voltage both at positive and negative source-drain voltage. (a) is positive gate, (b) is negative gate

(a)



(b)

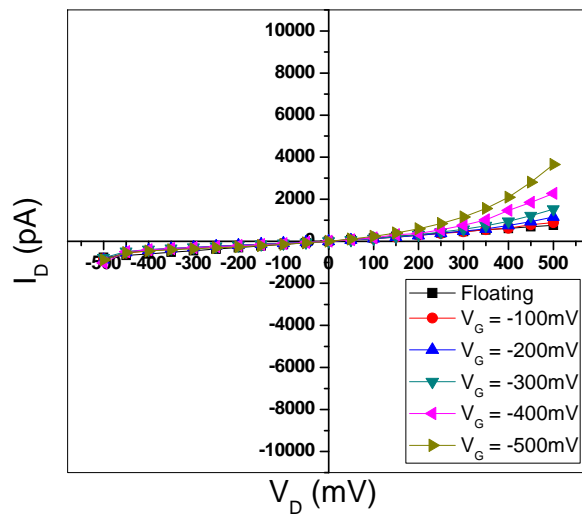
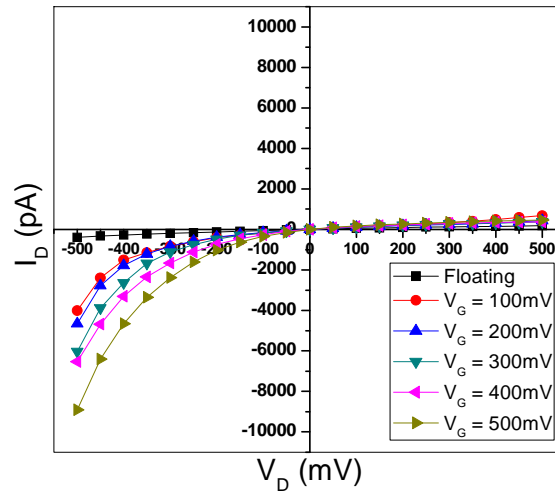


**Figure 4.3.** I-V graphs of the nanopore at 10mM KCl concentration. At this mole concentration, the rectification behavior can clearly be seen according to gate potential. Also, when the different gate voltage is applied, the rectification behavior is different depending on bias voltage. Rectification effect is larger under the positive gate voltage. (a) is positive gate, (b) is negative gate

(a)



(b)

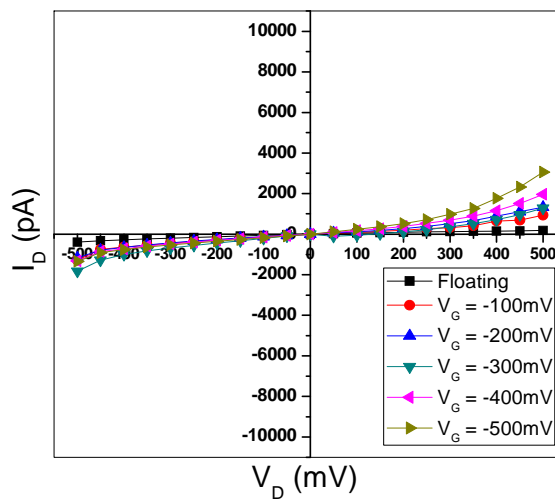


**Figure 4.4.** I-V graphs of the nanopore at 1mM KCl concentration. At this mole concentration, the rectification behavior can clearly be seen according to gate potential. Also, when the different gate voltage is applied, the rectification behavior is different depending on bias voltage. Rectification effect is larger under the positive gate voltage. (a) is positive gate. (b) is negative gate

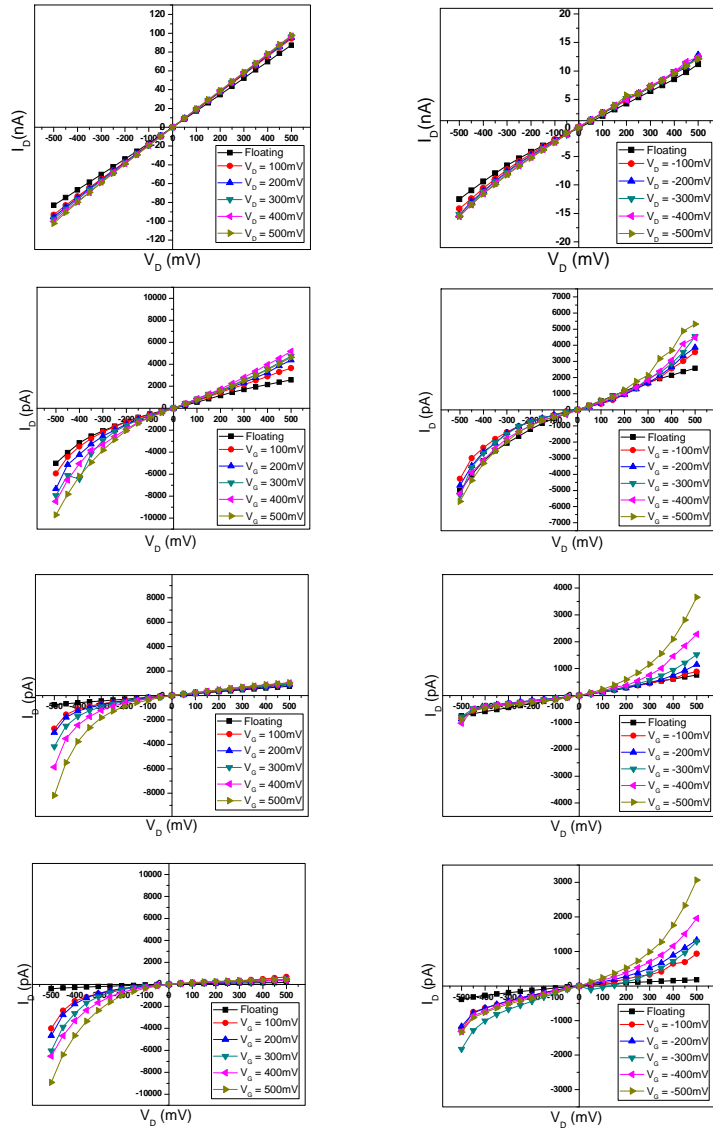
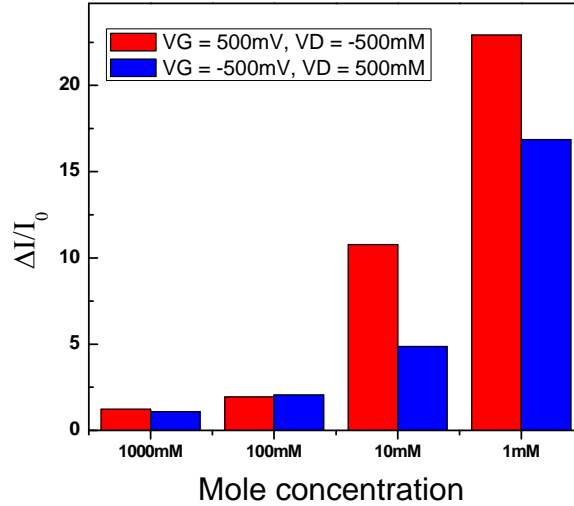


**Figure 4.5.** Overview of the results. The ionic current rectification depending on gate potential is shown according to mole concentration. The data is separated into two parts, positive (on the right side) and negative gate (on the left side). Here, the scale of ionic current is not adjusted as same in order to emphasize the rectification trend.

(a)



(b)

$\Delta I / I_0$	1M	100mM	10mM	1mM
+V <sub>G</sub> /+V <sub>D</sub>	1.12	1.79	1.38	2.52
+V <sub>G</sub> /-V <sub>D</sub>	1.23	1.94	10.77	22.92
-V <sub>G</sub> /-V <sub>D</sub>	1.24	1.13	1.17	3.44
-V <sub>G</sub> /+V <sub>D</sub>	1.08	2.06	4.80	16.86

**Figure 4.6.** The ratios of ionic current change to floating current are shown here. In order to compare the current change quantitatively, some values are extracted from the results. Every voltage value regardless of source-drain and gate voltage is the absolute 500mV. Graph(a) shows the current change according to mole concentration under the positive or negative gate voltage. The red bar is the positive gate and the blue bar is the negative gate. Graph(a) clearly shows that the ionic current increase with decrease of mole concentration and under the positive gate, the change is larger. Table (b) represents real values.

#### 4.2.2 Discussions

As explained in introductions part, breaking of symmetry in device geometry, ion concentration or surface charge is the major factor that causes the ionic current rectification effects, so finding out the asymmetric factor of the device is important for describing the results. First consideration is that our device has the asymmetrically positioned gate electrode and this layer is localized compare to the entire channel length and located at the relatively narrow region. The aluminum oxide deposited as the passivation layer has positive surface charge, so the negative ions are dominantly occupied in the nanopore at low mole concentration which means that the pore becomes anion selective. Thus, chlorine ions are the majority charge carrier and it is reasonable to take account only the anion into the explanation of ionic current behavior at low mole concentration. Under this situation, if the positive gate voltage is applied, negative ion concentration can be enhanced more than floating state, so around the gate region is much more anion selective. Hence, the gate region becomes literally “gate” to control the anion migration and inhibit the cation transportation then this anion reach region determines the ion flux.

Note that the data shows the ionic current enhancement when the positive gate and negative source-drain voltage is applied. Different polarity between gate and source-drain voltage generate larger potential gradients than same sign and then the majority charge carrier, negative ion, feel the stronger electric field. In order to screen out the electric field, the higher electric field result in the more ion concentration in the channel leading to increased ion flux. Because of all around gate, the

electric field caused by gate electrode is not formed onto the surface normal direction but lateral way. Therefore, negative source-drain voltage with positive gate potential makes plenty of electric field flux between electrodes leading the enhanced ionic current because carriers should move along the electric field line.

Also, we demonstrate the ratio of the ionic current change to the floating current according to mole concentration sweeping source-drain voltage (figure 4.7). In this figure, we can notice that the ionic current rectification is increased with decrease of mole concentration. Also, the Y-axis of the figure 4.7 is normalized by the ratio of the floating current to current change,  $\Delta I$ . From the data, the current enhancement is about 22 times higher than floating current under positive gate voltage and this is huge amount of change compare to other devices. The comparison with other devices will be shown in next section.

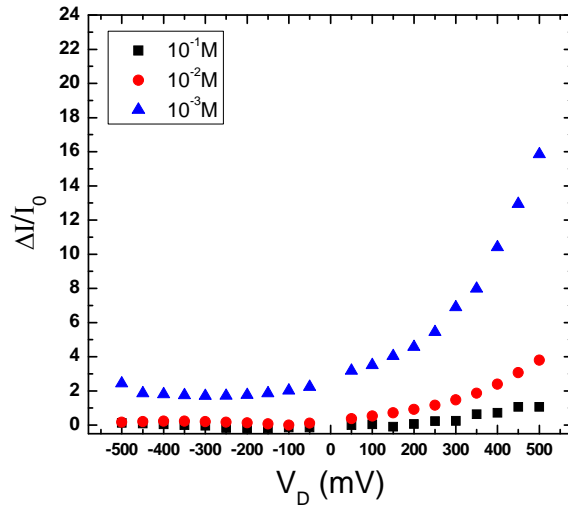
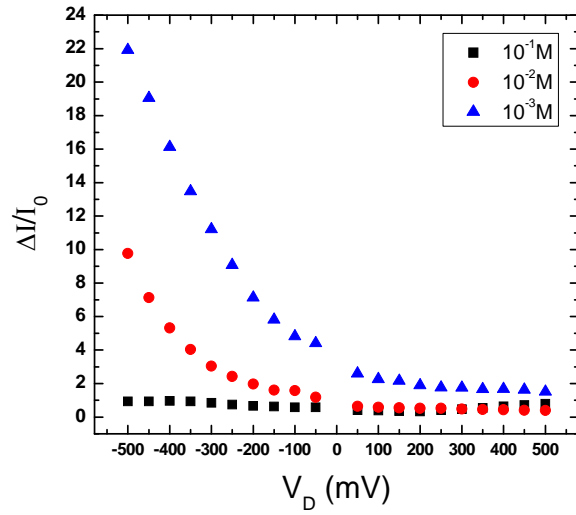


**Figure 4.7.** The ratio of ionic current change to floating current according to mole concentration. (a) is positive gate voltage and (b) is negative gate voltage. The maximum change is almost about 2200%. The gate voltage is +500mV and -500mV

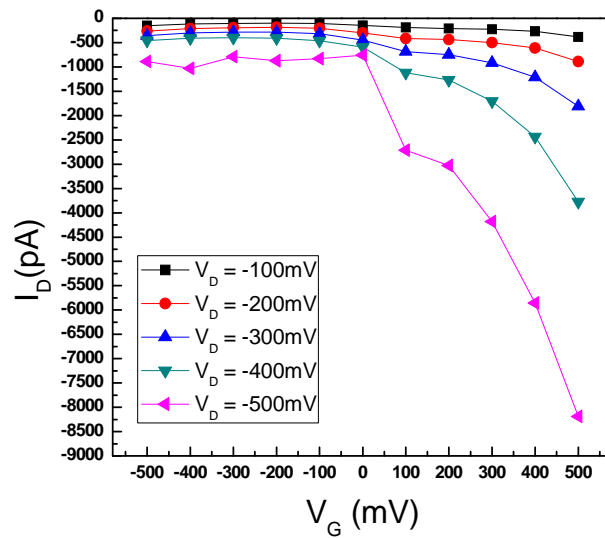
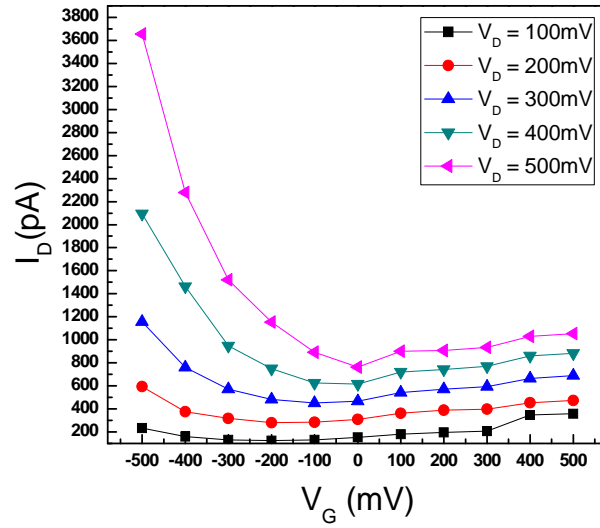


**Figure 4.8.**  $I_D$ - $V_G$  Graphs. The source drain voltage is separated into two parts; positive source-drain and negative source-drain voltage

### 4.3 Comparison analysis

In order to compare our results, some previous papers will be briefly reviewed. All of the papers show gate potential effect on ionic current. Each experiment was carried out under different conditions, so direct comparison is not possible. Thus, I decide that the maximum value of ionic current change or conductance change of each device is the criteria and compare each of them. First paper in figure 4.9 is reported in 2011 from Dereck Stein group. The 20nm nanopore used in the experiment was  $\text{Si}_3\text{N}_4$  pore with Cr gate electrode and the insulating layer was  $\text{Al}_2\text{O}_3$ . In this paper, they showed the  $\Delta I/I_0$  graph according to gate potential and the maximum change is about 0.1 at 1mM concentration.

Second paper in figure 4.10 suggests the field-effect reconfigurable nanofluidic ionic diodes which has nanochannel shape and asymmetrically positioned gate electrode. They used  $\text{SiO}_2$  trench as nanochannel that the height of the channel is about 20nm and length is about 100um. In this paper, the preferential current flow according to gate voltage was shown. But the current change is not so significant compare to our device. The maximum change of ionic current is shown in the figure 4.12.

The last paper in figure 4.11 reported the field-effect type nanopore system which can effectively modulate ion transport. This device has multiple nanopores with gate electrode. They showed the clear dependency of ionic current on gate potential and mole concentration. In this device, the author presented conductance changes according to mole concentration and the change begun to be appeared from 10mM

concentration. As can be seen in the figure, the ionic current rectification effect is the largest in our device compare to all other devices. Therefore, we can conclude that gate inserted nanopore with long thickness can modulate ion transport in very effective way and be an excellent ionic current rectification device.

In addition, one paper about numerical simulation of nanopore system is compared too. This group shows that a lot of parameters such as surface charge, position of gate electrode and gate potential can affect the ionic current rectification in conical nanopore with gate electrode systems. The modeling used in this paper is the above governing equation; Poisson equation and Nernst-Planck equation. Figure 4.13 (a) shows some of results from the paper and schematic image of the device structure for modeling. There are four graphs in figure 4.13(A) shows different I-V curves. (a) and (b) graph show the I-V data in case of mid positioned gate electrode. (c) and (d) graph show the I-V results in case of asymmetrically located gate on the tip side. Thus, we can compare the ion transport behavior according to gate electrode position. Also, (a) and (c) graph show the surface charge effects. The both red dashed line represent high surface charge and the black solid line is low surface charge. The symbols stand for ionic current under the gate potential. From the data, if the surface charge is high, the ionic current rectification takes place without gate voltage in both mid position and asymmetric position gate because the pore structure is very conical. Also, the surface charge is very high, there is no gate effect (red symbols). But in case of low surface charge, the floating current (solid black line) looks like ohmic behavior and also there are some current changes by gate potential (black symbols). Graph (b) and (d) in figure 4.13(A) shows the gate

effect on ion transport without any surface charge. In this graph, the surface charge is zero so this plot shows the gate controllability. Especially, the condition of simulation graph (b) is similar to our device because it has asymmetric pore size and gate electrode. But the graph (d) is that the gate electrode is located at the very near the tip region which is practically impossible to fabricate. Thus, we compared our experimental result and the simulation data and the two data is well matched (figure 4.13(b)). I believe that the difference between positive and negative gate which cannot be seen at the simulation is originated from the surface charge because the real device has certain amount of surface charge. The simulation data is for zero surface charge but in reality, perfect zero surface charge is impossible.

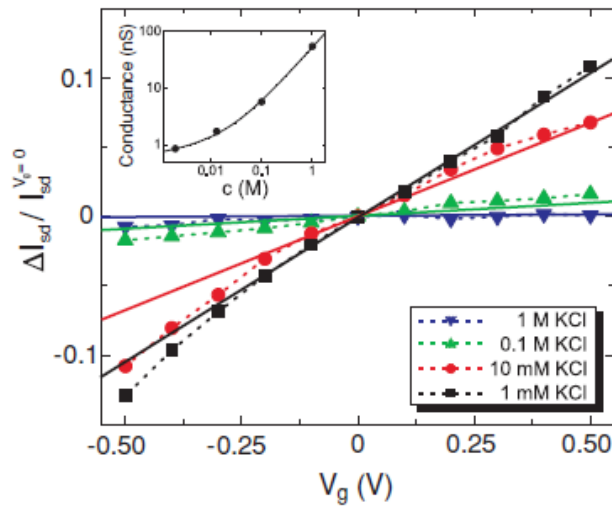
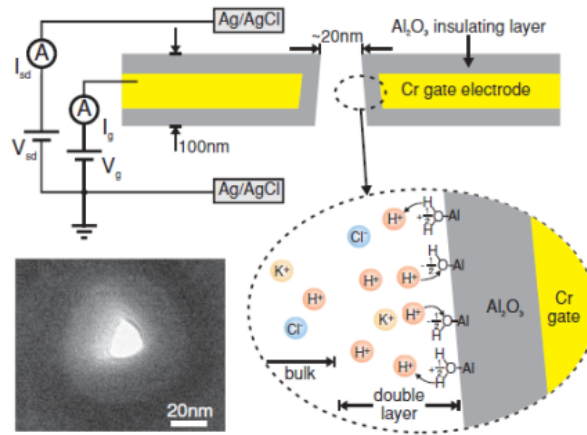
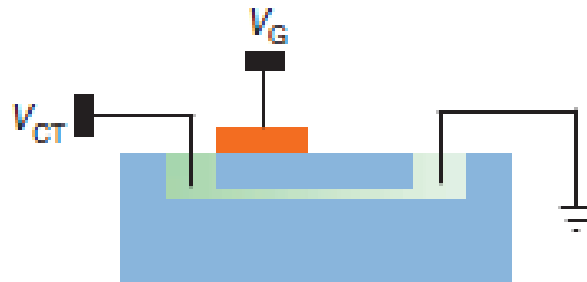


**Figure 4.9.** Device structure and ionic current change data. Nanopore on the Si<sub>3</sub>N<sub>4</sub> membrane with Cr gate has around 20nm diameter and is insulated by Al<sub>2</sub>O<sub>3</sub>. The graph shows the ratio of ionic current change to floating current according to gate voltage and the colors represent different mole concentration. Source-drain voltage was fixed as 200mV. The maximum value is about 0.1 at 1mM concentration.[1]

(a)



(b)

Field-effect reconfigurable diode

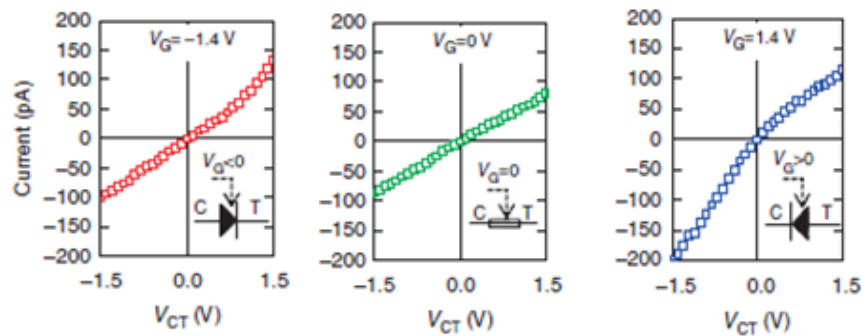


**Figure 4.10.** Field-effect reconfigurable nanofluidic ionic diodes and I-V plot. SiO<sub>2</sub> trench was used as nanochannels. The height, width and length of the channel is respectively, 20nm, 2μm and 100μm. Gate electrode was located asymmetrically at one side. The data I-V data show preferential ion flux according to bias voltage and the diode property is different according to gate bias.[2]

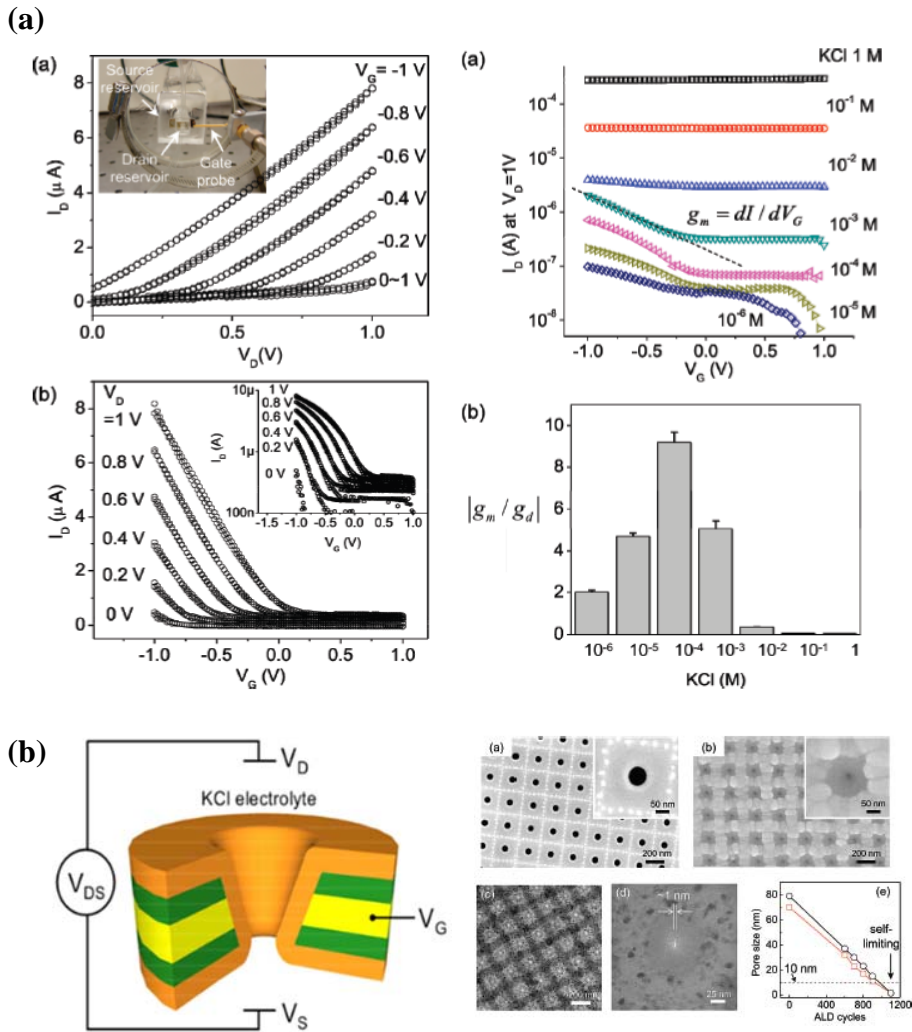
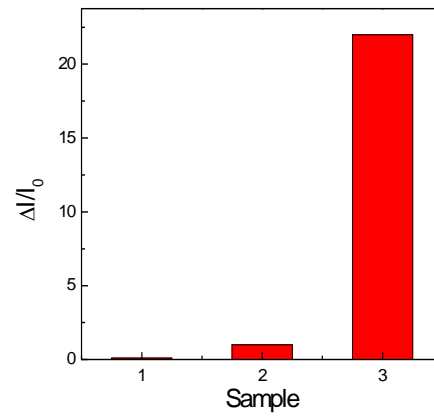


**Figure 4.11.** (a) Ionic transport of the nanopore IFET and gate modulation of ionic current for different KCl. (b) Schematic image of electrode-embedded nanopores for IFET and real device structure which shows multiple nanopores. The data shows clear change of ionic current according to gate voltage and the gate controllability according to mole concentration. From the results, this device has p-type like properties and the ionic current modulation is effective at the low electrolyte.[3]

(a)

	$\Delta I / I_0$
Derek Stein	0.1
Mark A. Reed	1
This work ( $V_{SD} = -500\text{mV}$ )	22
This work ( $V_{SD} = -200\text{mV}$ )	8



(b)

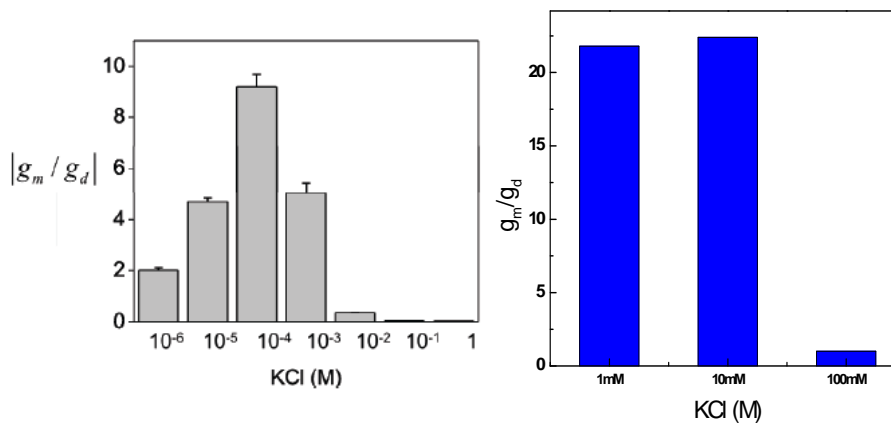
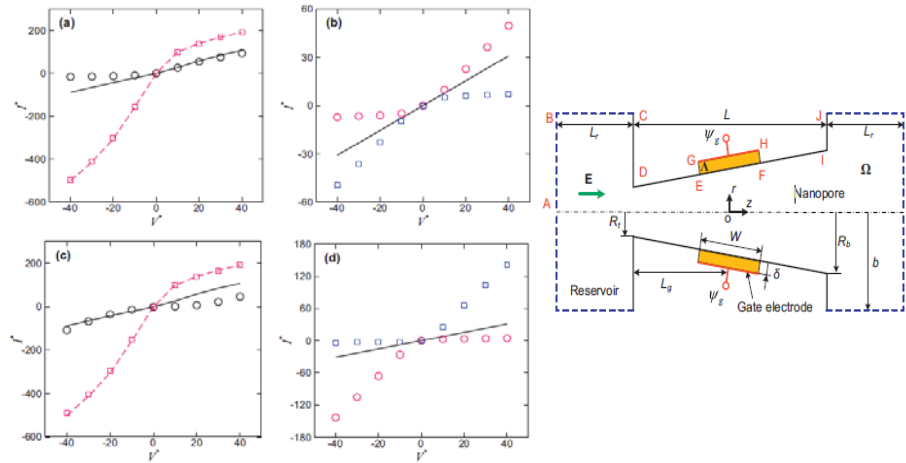


**Figure 4.12.** (a) The ratio of the current change to floating current is compared. The x-axis of the bar graph means each device and for convenience, number one, two and three represent respectively Derek Stein, Mark Reed and our group. From the data our device shows much effective ion modulation. (b) shows the conductance change compare to floating conductance. The one on the left side is Nam's data and the other is our data.[3]

(A)



(B)

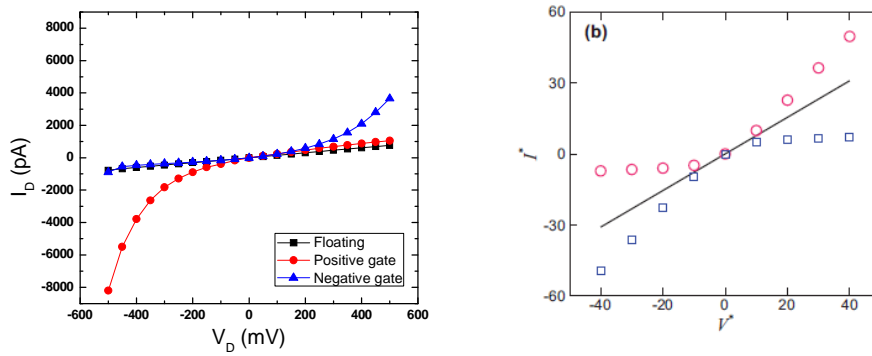


**Figure 4.13.** (A) The simulation data according to surface charge, gate position and gate voltage. (B) shows comparison the ionic current curve with the simulation data reported by Shizhi Qian at al. Red symbol represents positive gate and blue is negative gate. Source-drain voltage of the two data is applied in opposite way.[4]

#### 4.4 References

- 1 Jiang, Z. and D. Stein, *Charge regulation in nanopore ionic field-effect transistors*. Physical Review E, 2011. **83**(3).
- 2 Guan, W., R. Fan, and M.A. Reed, *Field-effect reconfigurable nanofluidic ionic diodes*. Nat Commun, 2011. **2**: p. 506.
- 3 Nam, S.-W., et al., *Ionic Field Effect Transistors with Sub-10 nm Multiple Nanopores*. Nano Letters, 2009. **9**(5): p. 2044-2048.
- 4 Ye Ai and Shizhi Qian, *Ionic current rectification in a conical nanofluidic field effect transistor*, Sensors and Actuators B. 2011. **157** p: 742-751
- 5 Siwy, Z.S., *Ion-Current Rectification in Nanopores and Nanotubes with Broken Symmetry*. Advanced Functional Materials, 2006. **16**(6): p. 735-746.
- 6 Cheng, L.-J. and L.J. Guo, *Rectified Ion Transport through Concentration Gradient in Homogeneous Silica Nanochannels*. Nano Letters, 2007. **7**(10): p. 3165-3171.
- 7 Daiguji, H., Y. Oka, and K. Shirono, *Nanofluidic Diode and Bipolar Transistor*. Nano Letters, 2005. **5**(11): p. 2274-2280.
- 8 Karnik, R., et al., *Rectification of Ionic Current in a Nanofluidic Diode*. Nano Letters, 2007. **7**(3): p. 547-551.
- 9 Fan, R., et al., *Polarity Switching and Transient Responses in Single Nanotube Nanofluidic Transistors*. Physical Review Letters, 2005. **95**(8).
- 10 Cheng, L.J. and L.J. Guo, *Nanofluidic diodes*. Chem Soc Rev, 2010. **39**(3): p. 923-38.
- 11 Stein, D., M. Kruithof, and C. Dekker, *Surface-Charge-Governed*

- Ion Transport in Nanofluidic Channels*. Physical Review Letters, 2004. **93**(3): p. 035901.
- 12 Daiguji, H., P. Yang, and A. Majumdar, *Ion Transport in Nanofluidic Channels*. Nano Letters, 2003. **4**(1): p. 137-142.
  - 13 Reto B. Schoch, *Transport phenomena in nanofluidics*. Rev Mod Phy, 2008. **80**(3): 6861
  - 14 G. Stell and C.G. Joslin, *The donnan equilibrium a theoretical study of the effects of interionic forces*. Biophysical society, 1986. **50**: p. 855-859
  - 15 W Sparreboom, *Transport in nanofluidic systems: a review of theory and applications*. New Journal of Physics, 2010. **12** p. 23
  - 16 Li-Jing Cheng and L. Jay Guo, *Rectified ion transport through concentration gradient in homogeneous silica nanochannels*, 2007. **7** p: 3165-3171
  - 17 Eric B. Kalman and Zuzanna S. siwy, *Control of ionic transport through gated single conical nanopores*, Anl Bioanal Chem, 2009. **394** 413-419

## **CHAPTER5. Summary and Conclusion**

In conclusion, we suggest the field effect type nanopore with all around gate electrode that shows the very effective controllability on ionic currents owing to its asymmetric structures of the nanopore. Also, this nanopore has very localized gate electrode compare to entire nanopore length which is different from the pre-existing nanochannels like mentioned in introduction. Broken symmetry of the nanopore is important role about the ionic current rectification indeed. Current enhancement and suppression of our device can be well matched with the established nanofluidic theories explained by using the total ion flux affected by several factors such as ion accumulation/depletion and electric potential. In addition, this result can be one proof of several numerical approaches. Therefore, this work will be able to provide the possibility of diverse biological and chemical applications which may need ionic current control. This very flexible and tunable nanofluidic device can open new ways to analyze, control, separate and transport biomolecules like DNA, RNA and proteins. Furthermore, for the lab-on-a chip application, our device can be an important contribution as a building block of the integrated chip.

## 국문초록

최근의 나노기술 분야의 놀라운 발전을 통해 소자 크기가 나노미터 수준으로 작아지게 되고 이에 따라 나노수력학(Nanofluidics)이라는 새로운 분야가 나타나게 되었다. 나노수력학은 나노미터 크기의 소자 내에 존재하는 물질들이나 유체에 대한 거동이나 조절에 대해 연구하는 분야이다. 여러 다양한 나노수력학 분야 중에서도 특별히 나노포어 및 나노채널은 생물학, 화학적 분석 및 검지를 위한 소자로써의 가능성으로 인해 많은 관심을 받고 있으며 이는 유체 환경 내에 존재하는 다양한 생물 분자들이나 나노입자와 같은 물질들을 다룰 수 있기 때문이다.

대표적인 이온 소자인 나노포어와 나노채널은 구조와 특성에 있어서 몇 가지 차이점을 가진다. 나노채널은 일반적으로 채널의 단면은 수십 나노미터 이하의 사이즈를 가지지만 채널의 길이는 수백 마이크로미터에 이르는 구조를 가지므로써 매우 큰 종횡비를 가지게 된다. 또한 수십 개의 채널이 배열을 이루는 구조를 가지고 있으며 이러한 수십 개의 채널들은 마이크로 채널과 함께 연결된 구조를 가지게 된다. 일반적으로 현재까지 보고된 결과에서는 나노채널 구조가 더 나은 이온 정류 효과를 가지는 것으로 보이며 또한 큰 종횡비를 가지는 구조 때문에 DNA와 같은 사슬 구조를 가지는 긴 분자들을 펼칠 수 있다는 장점이 있다. 이와 반면에 나노포어의 경우, 구조적으로는 상대적으로 매우 얇은 100nm이하의 두께를

가지며 10nm 이하의 매우 작은 나노포어 사이즈를 가진다. 또한 나노포어 소자는 소자내의 용액을 양분하는 멤브레인 구조를 가지고 있다. 나노포어는 이 멤브레인 상에 위치하게 되어 분자들이나 이온들이 통과하게 된다. 나노포어는 채널 소자에 비해 비교적 만들기 쉬운 공정과정을 가지며, 하나의 포어를 가지기 때문에 단 분자 분석에 좀 더 유용하다는 장점이 있다.

이러한 이온 소자들 중에 한가지 중요한 쟁점은 이온, 분자 혹은 나노입자와 같은 물질들의 이동현상을 이해하는 것이 중요한데, 이는 이러한 이동에 대한 이해가 우리가 목표로 하는 분자들을 조절하고 제어할 수 있게 해주기 때문이다. 따라서 이온 전류를 제어하는 것은 중요하다 할 수 있다. 반도체 소자와 유사하게 이온 소자에서도 선택적인 이온 Flux를 형성할 수 있는데, 이러한 선택적 흐름에 의해 발생하는 이온 전류 정류는 소자의 구조나, 소자 내부의 이온 농도와 같은 나노수력학적 시스템 내부에 비 대칭성이 존재할 때 발생하게 된다. 이러한 이온 전류 정류는 이온, 입자 그리고 생물학적 분자들을 선택적으로 이동시킬 수 있는 수단으로 여겨지고 있으며 따라서 좋은 정류 효과를 나타내는 소자를 만드는 것은 매우 중요하다.

이 논문에서 우리는 이온 정류 효과가 우수한 소자를 만들기 위해 3차원 구조를 가지는 Gate가 삽입된 나노포어를

만드는 공정을 제시한다. 여기서 나노포어 구조에 채널의 장점인 긴 이온 통로를 합쳐서 이온 정류 현상을 증가 시키고자 하였고, 따라서 나노포어의 구조는 상대적으로 일반적인 나노포어에 비해 매우 두꺼운 구조를 가지게 된다. 앞서 설명한 바와 같이 채널에서 더 우수한 정류현상을 나타낼 수 있으므로 두꺼운 구조를 채택하였으며, 또한 정류현상의 핵심인 소자 내부에 존재하는 나노수력학적 비 대칭성을 증가시키기 위하여 아래, 위쪽의 포어 사이즈를 달리 하였으며, Gate 층 역시 비대칭적으로 삽입을 하였다. 이 연구에서의 소자 특성이 논문을 통해 소개 될 것이며, 우리는 본 논문에 소개된 나노포어가 매우 우수한 Gate 제어성을 보여 줄 수 있을 것으로 기대한다.

**Keywords:** Ionic current rectification, Nanopores, Gate

**Student number:** 2012-22538

## Acknowledgement (in Korean)

### 감사의 글

설렘과 기대로 입학한지가 엇그제 같은데 벌써 2년이 라는 시간이 흘러 석사 졸업시기가 다가 온 것을 보니 시간이 참 빠르게 가는 것 같습니다. 나노공정 연구실에서의 2년은 저의 20대 시절 중 가장 치열하고 도전적이었던 시간이었던 것 같습니다. 훌륭한 교수님들과 선배, 동료들을 통해서 연구가 무엇인지 조금이지만 배울 수 있었고, 2년간의 연구를 통해서 작지만 무엇인가를 성취한다는 것이 어떤 것인지 배울 수 있어 감사한 시간이었습니다. 저의 지난 2년 간을 함께하며 여러 방면으로 도와주신 여러분들께 감사의 글을 전하고자 합니다.

우선 저의 지도 교수님이신 김기범 교수님께 깊은 감사의 말씀을 드립니다. 저에게 연구자로서 어떠한 마음가짐을 가지고 살아야 하는지 알려주시고 어려운 주제로 고민하며 일이 잘 진척이 되지 않을 때도 스승님의 마음으로 기다리고 지도해주셔서 지금의 자리에 있을 수 있게 되었습니다. 실험을 하면서 겪게 되는 많은 어려움들 속에서 문제들을 어떻게 바라보며, 어떻게 체계적이면서도 논리적인 방법으로 접근해 풀어가야 하는지 알려주신 교수님의 가르침을 항상 기억하도록 노력하겠습니다. 교수님의 가르침과 도움으로 얻게 된 것은 단순한 실험적 결과뿐만이 아닌, 생각하는 방법과 생각을 전개해

나가는 방법이었습니다. 지도교수님께 깊은 감사의 마음을 전합니다. 또한 전기·정보 공학부의 김성재 교수님께도 감사의 말씀을 드립니다. 교수님을 통해 생소하던 Nanofluidic 분야에 대한 개념을 잡을 수 있었고 또한 기꺼이 시간을 허락해주셔서 실험 결과에 대한 의미 있는 논의들을 가질 수 있게 해주신 점은 진심으로 감사 드립니다. 교수님과의 논의를 통한 다양한 해석들이 저의 연구에 많은 영향을 미쳤고, 도움을 얻을 수 있었기에 감사의 마음을 전합니다. 또한 바쁘신 와중에도 저의 졸업 심사를 맡아주신 홍성현 교수님과 님기태 교수님께도 감사 드립니다. 교수님들께서 심사 때 해주신 연구 결과에 대한 조언들과 격려의 말씀에 감사 드립니다.

그리고 2년간 저의 삶의 가장 많은 시간을 함께 나누었던 나노공정 연구실 구성원들께도 감사의 말씀을 전하고 싶습니다. 제가 이 곳에 잘 적응하고 졸업할 수 있었던 것 중에 가장 중요한 이유 중 하나가 바로 가족같이 화목한 연구실 분위기라고 생각합니다. 실험실 여러분들과의 인연이야말로 이 곳에서 얻은 가장 큰 자산이 아닐까 합니다.

먼저 현미누나에게 감사의 말씀드립니다. 누나가 저를 위해 보이는 곳에서 보이지 않는 곳에서 도와주신 점 잘 알고 있고 깊이 감사합니다. 힘든 시간들이 있을 때 도 누나의 도움이 정말 컸었습니다. 제일 어른으로써 저뿐만 아니라 모든 학생들을 생각해주시고 신경 써 주셔서 감사합니다. 연구에 있어서도 도움을 요청하면 기꺼이 도와주시고, 자료를 해석하고 그

를 통해 논리를 만들어가는 과정에 대해 아낌없이 도움을 주셔서 감사합니다. 근면한 모습으로 후배들에게 모범이 되셨던 도중이 형. 맡고 있는 연구에 대한 형의 진지함과 성실함을 통해 많은 도전을 받았고 또, 연구 할 때는 진지하시지만 여행을 가셨을 때나 후배들과의 회식자리에서 소탈하고 진솔한 모습을 보여주셨던 시간들이 생각납니다. 미국에서 새로운 도전을 펼치고 계시는 형님 잘 해내시리라 믿고 늘 건승 하시기를 바랍니다. 나노포어 팀의 가장 큰 선배님이었던 민현이 형 감사합니다. 나노포에 대해 아무것도 모르던 제가 형을 통해서 많은 도움을 얻을 수 있었습니다. 특히 공정하는 부분에 있어서 많은 도움을 주셔서 감사합니다. 형의 도움으로 소자를 완성할 수 있었습니다. 그리고 승우형, 짧은 시간 함께 했지만 여행과 술자리에서 즐거운 모습 보여주시고 편안하게 해주셔서 연구실에 빨리 잘 적응할 수 있었습니다. 지금은 졸업하고 없지만 함께 즐거운 시간을 보냈던 기용이와 민이에게도 고맙습니다. 서로 어떤 주제에 대해 연구하는지를 떠나서 항상 편안하고 친밀하게 대해 줘서 고맙습니다. 기용이는 늦은 나이에 군대를 가게 되어서 많이 힘들었을 텐데 다행히 최근에는 군생활이 제가 있을 때 보다 많이 즐기고 또 환경도 많이 좋아졌다고 하니 무사히 잘 전역하리라 생각하고, 전역 후에도 원하는 일 잘 해나가길 바랍니다. 민이는 상냥한 성격 덕분에 대화를 나눌 때 편안하고 가끔 말 동무가 되어 즐거웠습니다. 언제나 활기차고 즐거운 모습을 모셨던 재일이도 생각납니다. 공과대학교 대학원에 있는 연구실은 웬지 사람들이 연구 주제에

대해서만 이야기 할 것 같은 무거운 분위기였지만 그게 아니라 하는 것을 몸소 보여준 재일이. 언제나 주위 사람들을 즐겁게 해주는 좋은 성격 덕분에 짧은 시간이었지만 힘들었던 첫 학기를 즐겁게 보낼 수 있어 고맙습니다. 최근에 몸이 많이 아팠는데 얼른 건강회복하고 계획하는 모든 일에 다 승승장구 하길 바랍니다. 그리고 현재 학생들 중 제일 연장자이신 승현이 형 에게도 감사 드립니다. Gate구조를 한다는 이유만으로 여러 방향으로 경험할 수 있게 도와주고, 자기 일처럼 저의 연구에 관심을 가져주셔서 감사했습니다. 동갑이지만 머나먼 선배님이신 성용이 에게도 많이 고맙습니다. 아무것도 모르던 1학년때 좋은 SEM을 찍을 수 있게 도와줘서 졸업 연구결과를 위한 좀 더 탄탄한 근거를 만들 수 있었습니다. 실험 외적으로도 물심양면 도와주었던 부분에 대해서도 고맙습니다. 안타깝게도 정해진 기한 내에 좋은 결과를 얻진 못하였지만 그래도 많은 도움을 얻었고 또 다음에 기회가 있을 거라 생각합니다. 때론 유쾌하고 때론 진지하게 조언해주는 기주형에게도 감사합니다. 형이 제공해 주신 유용한 정보들은 가슴 깊이 새겨두어 여자 친구와 함께 잘 누리도록 하겠습니다. 나노포어팀 선배인 경범이도 고맙습니다. 경범이가 나노포어 관련 실험에 대해 기초부터 잘 알려주었기 때문에 연구를 잘 해올 수 있지 않았나 합니다. 도움을 요청하거나 질문을 하면 하던 일도 멈추고 도와줘서 고마운 선배였습니다. 동기였던 지연이와 형준에게도 고맙습니다. 친목을 위해 동기끼리 함께 에버랜드에 가서 즐거운 시간을 보냈던 때가 기억나네요. 동기로써 함께 서

로 서로 챙겨 줄 수 있어서 행복했었습니다. 한 한기 늦게 들어온 천광이 형과 홍식이기도 함께 해서 즐거웠습니다. 대화를 하면 항상 진솔하게 임해주던 천광이 형이 생각납니다. 유머러스하고 유쾌한 홍식이와 장난을 주고 받던 것이 생각 나네요. 홍식이 덕분에 연구실 생활이 즐거웠습니다 왜냐하면 홍식이 때문에 즐거웠기 때문이지요. 이번에 새롭게 들어온 상훈이를 포함해 기단이, 영호, 민수, 재현이, 그리고 재석에게도 고맙습니다. 그냥 후배 존재만으로도 좋은 것 같습니다. 성격 좋고 똑똑한 후배들 덕분에 마지막 1년 동안 힘들 때도 즐겁게 보낼 수 있었습니다. 좋은 차를 자주 권유해 주던 기단이 덕분에 목 감기가 걸렸을 때 도움을 받아 고맙습니다. 자신 있고 당돌한 영호는 무슨 일을 하더라도 거뜰히 해낼 수 있으리라 믿습니다. 아련한 고향이 떠오르게 하는 말투를 가진 민수도 부족한 선배이지만 잘 따라 주어 고맙고 많이 도와주지 못해 미안한 마음이 듭니다. 새롭게 옮긴 팀에서 건승하시길 바랍니다. 듬직한 재현이도 어려운 나노채널 연구를 하는데 묵묵히 자기 일을 하는 것을 보면 좋은 결과를 얻을 수 있을 것 같습니다. 성격 좋고 신사다운 재석이기도 알게 되어 좋습니다. 연구실에 청소나 기타 굵은 잡일이 있을 때 늘 솔선수범하는 모습을 보고 칭찬 하고 싶었는데 이 글을 통해서 겨우 하게 되네요. 마지막으로 떠나면 타국인 한국에 와서 열심히 연구하고 있는 아슈도 2년간 함께 할 수 있어 즐거웠습니다. Kumar, it was a great time to be with you for the last two years. I hope all is well with you and your family. 또한 연구실에 없어서는 안될 밝은 미소의

혜진이 누나와 정은이에게도 감사의 마음 전합니다. 최근에 득남하셨는데 아기가 무척 귀엽더군요. 육아와 학교일 병행이 쉽지 않겠지만 항상 힘내시기 바랍니다. 열심히 나노포어 사진을 찍어 준 정은이도 많이 고맙습니다. 정은이 덕분에 실험을 잘 할 수 있었습니다. 저의 2년을 기쁨과 감사로 채워 주신 여러 연구실 동료 분들 모두에게 전심으로 감사의 마음 전합니다.

마지막으로 저의 가족에게 감사의 마음을 전합니다. 아들이 이 자리에 있기까지 사랑하는 부모님의 도움이 없었다면 저는 이 곳에 있을 수 없었을 것입니다. 제 인생의 모든 성취와 누리는 모든 행복들은 부모님 없이는 설명할 수 없습니다. 농촌에서 힘들게 일하시는 부모님 항상 건강하시고, 두분 오래 오래 서로 행복하고 사랑하시길 기도합니다. 또한 사랑하는 동생도 늘 건강하고 부지런히 노력하여서 좋은 미래를 성취하기 바란다. 어머니, 아버지 사랑합니다. 여자 친구도 늘 곁에서 힘이 되어 줘서 고마워.

나의 전부이자, 살아가는 이유이며, 살아내야만 하는 이유이고, 힘들 때 도움이시고, 슬플 때 위로이시며, 인생의 인도자 이시며, 나의 생명이 되시는 하나님께, 그리고 예수님께 저의 모든 마음을 다하여 감사 드리고 영광 돌립니다. Soli Deo Gloria!

2014년 1월 14일 여정모